ACKNOWLEDGMENTS

The author thanks all the member of the division of Cellular and Molecular Toxicology, NIHS for strong support of the project, and Dr. Bruce Blumberg for critical reading of the manuscript. The project has been supported by MHLW Health Sciences Research Grants H24-Kagaku-Shitei-006, H21-Kagaku-Ippan-001, H19-Toxico-001, H18-Kagaku-Ippan-001, H15-Kagaku-002, H14-Toxico-001, and H13-Seikatsu-012.

REFERENCES

Braun, W.H., Young, J.D., Blau, G.E. and Gehring, P.J. (1977): The pharmacokinetics and metabolism of pentachlorophenol in rats. Toxicol. Appl. Pharmacol., **41**, 395-406.

Carignan, D., Désy, O. and de Campos-Lima, P.O. (2011): The dysregulation of the monocyte/macrophage effector function induced by isopropanol is mediated by the defective activation of distinct members of the AP-1 family of transcription factors. Toxicol. Sci., **125**, 144-156.

Clayton, G.D. and Clayton, F.E. (1981): Toxicology. John Wiley Sons, New York.

Damm, J., Wiegand, F., Harden, L.M., Gerstberger, R., Rummel, C. and Roth, J. (2012): Fever, sickness behavior, and expression of inflammatory genes in the hypothalamus after systemic and localized subcutaneous stimulation of rats with the Toll-like receptor 7 agonist imiquimod. Neuroscience, **201**, 166-183.

Deichman, W., Machle, W., Kitzmiller, K.V. and Thomas, G. (1942): Acute and chronic effects of pentachlorophenol and sodium pentachlorophenate upon experimental animals. J. Pharmacol. Exp. Ther., **76**, 104-117.

Dinarello, C.A. (1999): Cytokines as endogenous pyrogens. J Infect Dis., **179 Suppl. 2**, S294-S304.

Finck, B.N., Gropler, M.C., Chen, Z., Leone, T.C., Croce, M.A., Harris, T.E., Lawrence, J.C.Jr. and Kelly, D.P. (2006): Lipin 1 is an inducible amplifier of the hepatic PGC-1alpha/PPARalpha regulatory pathway. Cell. Metab., **4**, 199-210.

Gomard, T., Michaud, H.A., Tempé, D., Thiolon, K., Pelegrin, M. and Piechaczyk, M. (2010): An NF-kappaB-dependent role for JunB in the induction of proinflammatory cytokines in LPS-activated bone marrow-derived dendritic cells. PLoS One, **5**, e9585.

Hemmi, H., Kaisho, T., Takeuchi, O., Sato, S., Sanjo, H., Hoshino, K., Horiuchi, T., Tomizawa, H., Takeda, K. and Akira, S. (2002): Small anti-viral compounds activate immune cells via the TLR7 MyD88-dependent signaling pathway. Nat. Immunol., **3**, 196-200.

Jung, J., Ishida, K. and Nishihara, T. (2004): Anti-estrogenic activity of fifty chemicals evaluated by in vitro assays. Life Sci., **74**, 3065-3074.

Kanno, J., Aisaki, K., Igarashi, K., Nakatsu, N., Ono, A., Kodama, Y. and Nagao, T. (2006): "Per cell" normalization method for mRNA measurement by quantitative PCR and microarrays. BMC Genomics, **7**, 64.

Kawaguchi, M., Morohoshi, K., Saita, E., Yanagisawa, R., Watanabe, G., Takano, H., Morita, M., Imai, H., Taya, K. and Himi, T. (2008): Developmental exposure to pentachlorophenol affects the expression of thyroid hormone receptor beta1 and synapsin I in brain, resulting in thyroid function vulnerability in rats. Endocrine, **33**, 277-284.

Konishi, H., Okamoto, K., Ohmori, Y., Yoshino, H., Ohmori, H., Ashihara, M., Hirata, Y., Ohta, A., Sakamoto, H., Hada, N., Katsume, A., Kohara, M., Morikawa, K., Tsukuda, T., Shimma, N., Foster, G.R., Alazawi, W., Aoki, Y., Arisawa, M. and Sudoh, M. (2012): An orally available, small-molecule interferon inhibits viral replication. Sci. Rep., **2**, 259.

Larsen, R.V., Kirsch, L.E., Shaw, S.M., Christian, J.E. and Born, G.S. (1972): Excretion and tissue distribution of uniformly labeled 14 C-pentachlorophenol in rats. J. Pharm. Sci., **61**, 2004-2006.

Lucas, K. and Maes, M. (2013): Role of the Toll Like Receptor (TLR) Radical Cycle in Chronic Inflammation: Possible Treatments Targeting the TLR4 Pathway. Mol. Neurobiol., (in press).

NTP (1999): NTP Toxicology and Carcinogenesis Studies of Pentachlorophenol (CAS NO. 87-86-5) in F344/N Rats (Feed Studies). In: Natl Toxicol Program Tech Rep Ser), pp.1-182.

Ohnishi, T., Yoshida, T., Igarashi, A., Muroi, M. and Tanamoto, K. (2008): Effects of possible endocrine disruptors on MyD88-independent TLR4 signaling. FEMS Immunol. Med. Microbiol., **52**, 293-295.

Puigserver, P., Rhee, J., Donovan, J., Walkey, C.J., Yoon, J.C., Oriente, F., Kitamura, Y., Altomonte, J., Dong, H., Accili, D. and Spiegelman, B.M. (2003): Insulin-regulated hepatic gluconeogenesis through FOXO1-PGC-1alpha interaction. Nature, **423**, 550-555.

Sato, M., Suemori, H., Hata, N., Asagiri, M., Ogasawara, K., Nakao, K., Nakaya, T., Katsuki, M., Noguchi, S., Tanaka, N. and Taniguchi, T. (2000): Distinct and essential roles of transcription factors IRF-3 and IRF-7 in response to viruses for IFN-alpha/beta gene induction. Immunity, **13**, 539-548.

Tasaki, M., Kuroiwa, Y., Inoue, T., Hibi, D., Matsushita, K., Ishii, Y., Maruyama, S., Nohmi, T., Nishikawa, A. and Umemura, T. (2012): Oxidative DNA damage and *in vivo* mutagenicity caused by reactive oxygen species generated in the livers of p53-proficient or -deficient gpt delta mice treated with non-genotoxic hepatocarcinogens. J. Appl. Toxicol. DOI: 10.1002/jat.2807.

Zhu, B.Z. and Shan, G.Q. (2009): Potential mechanism for pentachlorophenol-induced carcinogenicity: a novel mechanism for metal-independent production of hydroxyl radicals. Chem. Res. Toxicol., **22**, 969-977.

The web site for GeneChip data

The GeneChip data of PCP are accessible at http://www.nihs.go.jp/tox/TtgPublished.htm

Bone 60 (2014) 68–77

Contents lists available at ScienceDirect

Bone

journal homepage: www.elsevier.com/locate/bone

Original Full Length Article

Estrogen receptor α in osteocytes regulates trabecular bone formation in female mice

Shino Kondoh [a], Kazuki Inoue [a,b,c], Katsuhide Igarashi [d], Hiroe Sugizaki [e], Yuko Shirode-Fukuda [a], Erina Inoue [a], Taiyong Yu [a,b], Jun K. Takeuchi [e,f], Jun Kanno [d], Lynda F. Bonewald [g], Yuuki Imai [a,b,*]

[a] Laboratory of Epigenetic Skeletal Diseases, Institute of Molecular and Cellular Biosciences, The University of Tokyo, Tokyo, Japan
[b] Division of Integrative Pathophysiology, Proteo-Science Center, Graduate School of Medicine, Ehime University, Ehime, Japan
[c] Department of Biological Resources, Integrated Center for Science, Ehime University, Ehime, Japan
[d] Division of Cellular & Molecular Toxicology, Biological Safety Research Center, National Institute of Health Sciences, Tokyo, Japan
[e] Division of Cardiovascular Regeneration, Institute of Molecular and Cellular Biosciences, The University of Tokyo, Tokyo, Japan
[f] JST PRESTO, Japan
[g] Department of Oral Biology, School of Dentistry, University of Missouri at Kansas City, Kansas City, MO, USA

ARTICLE INFO

Article history:
Received 8 July 2013
Revised 26 November 2013
Accepted 4 December 2013
Available online 10 December 2013

Edited by: Shu Takeda

Keywords:
Estrogen
Estrogen receptor α
Osteocyte
Bone formation
Wnt signaling

ABSTRACT

Estrogens are well known steroid hormones necessary to maintain bone health. In addition, mechanical loading, in which estrogen signaling may intersect with the Wnt/β-catenin pathway, is essential for bone maintenance. As osteocytes are known as the major mechanosensory cells embedded in mineralized bone matrix, osteocyte ERα deletion mice ($ER\alpha^{\Delta Ocy/\Delta Ocy}$) were generated by mating ERα floxed mice with Dmp1-Cre mice to determine the role of ERα in osteocytes. Trabecular bone mineral density of female, but not male $ER\alpha^{\Delta Ocy/\Delta Ocy}$ mice was significantly decreased. Bone formation parameters in $ER\alpha^{\Delta Ocy/\Delta Ocy}$ were significantly decreased while osteoclast parameters were unchanged. This suggests that ERα in osteocytes exerts osteoprotective function by positively controlling bone formation. To identify potential targets of ERα, gene array analysis of Dmp1-GFP osteocytes sorted by FACS from $ER\alpha^{\Delta Ocy/\Delta Ocy}$ and control mice was performed. Gene expression microarray followed by gene ontology analyses revealed that osteocytes from $ER\alpha^{\Delta Ocy/\Delta Ocy}$ highly expressed genes categorized in 'Secreted' when compared to control osteocytes. Among them, expression of Mdk and Sostdc1, both of which are Wnt inhibitors, was significantly increased without alteration of expression of the mature osteocyte markers such as Sost and β-catenin. Moreover, hindlimb suspension experiments showed that trabecular bone loss due to unloading was greater in $ER\alpha^{\Delta Ocy/\Delta Ocy}$ mice without cortical bone loss. These data suggest that ERα in osteocytes has osteoprotective functions in trabecular bone formation through regulating expression of Wnt antagonists, but conversely plays a negative role in cortical bone loss due to unloading.

Published by Elsevier Inc.

Introduction

Estrogens clearly maintain physiological homeostasis through the development of reproductive organs and the mammary gland, potentiation of muscles, and through osteoprotection. The osteoprotective actions of estrogens are clearly demonstrated by post-menopausal osteoporosis [1]. The effects of sex steroid hormones on bone tissue can be considered as the combination or sum of the direct effects on bone cells and the indirect effects on other tissues [2]. The indirect effects of estrogen on bone through other tissues have been well described, such as modulation of cytokine production by immune cells and the increased induction of pituitary gland hormones [3,4]. However, the direct effect of estrogens on bone tissue is not fully understood.

Estrogens exert their effects by binding to their own nuclear receptors, such as Estrogen Receptor (ER) α and β, which also function as transcription factors. The conventional ERα null mouse model could not be used to address the direct functions of the receptor in bone due to hormonal imbalance and endocrine disturbances [5–7]. Therefore, the generation and analyses of bone cell type specific deletion is required to clarify the functions of ERα in bone.

Osteoclastic ERα null mice were generated showing that osteoclastic ERα shortens the life span of osteoclasts by promoting apoptosis [8,9]. Ovariectomy can induce osteocyte apoptosis [10] and conventional ERα null mice do not increase bone mass in response to anabolic mechanical loading [11]. Moreover, various groups reported murine skeletal phenotype due to ERα deletion in cells of the osteoblast lineage, suggesting ERα in osteoblastic lineage cells could play important roles in the maintenance of bone metabolism [12–15]. Recently, Windahl

* Corresponding author at: Division of Integrative Pathophysiology, Proteo-Science Center, Graduate School of Medicine, Ehime University, Shitsukawa, Toon, Ehime 791-0295, Japan. Tel.: +81 89 960 5925; fax: +81 89 960 5953.
E-mail address: y-imai@m.ehime-u.ac.jp (Y. Imai).

8756-3282/$ – see front matter. Published by Elsevier Inc.
http://dx.doi.org/10.1016/j.bone.2013.12.005

et al. [13] reported that ERα in osteocytes regulates trabecular bone formation and thus trabecular bone volume in male mice. These results are in contrast to our own findings showing that the precise molecular functions and target genes of ERα in osteocytes still remain elusive.

Osteocytes are embedded in the extracellular matrix of bone and represents more than 90% of the cells existing in bone. Osteocytes possess dendrites that extend throughout the bone and are used to communicate with each other and also with osteoblasts and osteoclasts on the surface of the bone. The function of osteocytes as mechanosensory cells is inferred from their shape and location [16]. In fact, mechanical loading and unloading change osteocyte gene expression *in vivo*, indicating that osteocyte function is affected by loading conditions [17–20]. In addition, they are known to be involved in mineral metabolism through expression of proteins such as FGF23, Phex, Mepe, and Dmp1 [21–24] (for review, see [25]). Recently, it has been postulated that osteocytes can orchestrate skeletal homeostasis through mineral metabolism as well as the regulation of osteoblastic bone formation and osteoclastic bone resorption by secretory proteins such as sclerostin and FGF23. Osteocytes are also reported to regulate osteoblastic bone formation through IGF-1, TGFβ, NO, PGE_2 and sclerostin and to regulate osteoclastic bone resorption through TGFβ, NO, and PGE_2, and RANKL/OPG [26].

Bone mass can be maintained by mechanical loading while unloading or immobilization decreases bone mass. *In vivo* unloading rodent models such as tail suspension can induce bone loss in hind limbs [27] and mechanical loading can increase bone mass in forelimbs [28]. The regulation of bone mass by mechanical loading is mediated, at least in part, through β-catenin signaling [29–31], and estrogen/ER signaling might also be involved in this mechanism [32].

In this study, we examined the functions of ERα in osteocytes by generating mice lacking ERα in osteocytes and analyzing osteocyte gene expression profiles and subjecting them to hindlimb unloading.

Materials and methods

Animals

The ERα floxed mutant ($ER\alpha^{L2/L2}$) mice kindly provided by Dr. Chambon and null alleles with a C57BL/6 J background have been previously described [5]. $ER\alpha^{L2/L2}$ mice were crossed with $Dmp1^{Cre}$ mice [33] to generate $Dmp1^{Cre}$; $ER\alpha^{L2/+}$ mice, and $Dmp1^{Cre}$; $ER\alpha^{L2/L2}$ ($ER\alpha^{\Delta Ocy/\Delta Ocy}$) and $ER\alpha^{L2/L2}$ ($ER\alpha^{flox/flox}$) were obtained by crossing $Dmp1^{Cre}$; $ER\alpha^{L2/+}$ and $ER\alpha^{L2/L2}$. *Dmp1-GFP* mice were kindly provided by Dr. Ivo Kalajzic [34]. All mice were housed in a specific-pathogen-free facility under climate-controlled conditions with a 12-hour light/dark cycle and were provided with water and standard diet (CE-2, CLEA, Japan) *ad libitum*. All animals were maintained and examined according to the protocol approved by the Animal Care and Use Committee of the University of Tokyo.

Genome DNA extraction and cell culture

Various tissues (0.5 g) from $ER\alpha^{\Delta Ocy/\Delta Ocy}$ were harvested, washed with PBS and lysed in 2 ml of lysis buffer with proteinase K (150 μg/ml) overnight. Also, DNA of osteocytes was isolated from the calvariae of $ER\alpha^{\Delta Ocy/\Delta Ocy}$ in which cells on the surface of the bone such as osteoclasts and osteoblasts were removed by sequential enzymatic treatment. Primary osteoblasts obtained from the neonatal calvariae were cultured in αMEM (Life Technologies) containing 10% FBS (Cell Culture Bioscience), 50 μg/ml ascorbic acid (Sigma-Aldrich) and 10 nM β-glycerophosphate (Sigma-Aldrich) for 21 days. Cells were cultured with phenol red free media 24 h before cells were treated with 17β-estradiol. Primary osteoclasts were differentiated from the bone marrow obtained from 6-week-old $ER\alpha^{\Delta Ocy/\Delta Ocy}$ mice using 10 ng/ml of M-CSF (R&D Systems) and 234 ng/ml of GST-RANKL (Oriental Yeast) for 5 days. The genomic DNA was extracted using phenol/chloroform and isopropanol precipitation.

ELISAs

Enzyme-linked Immunoassays, ELISAs, were was performed following the protocols of the Estradiol EIA Kit (Cayman Chemical Company) for estradiol, Testosterone EIA Kit (Cayman Chemical Company) for testosterone, and Rodent Luteinizing Hormone (LH) ELISA TEST (Endocrine Technologies) for LH.

Bone analyses

The BMD of femurs and tibiae obtained from 12-week-old littermates were measured by DXA using a bone mineral analyzer (DCS-600EX: ALOKA). Micro Computed Tomography scanning of the tibiae and femurs was performed using a Scanco Medical μCT35 System (SCANCO Medical) with an isotropic voxel size of 6 μm for trabecular analyses and 12 μm for cortical analyses according to the manufacturer's instructions and the recent guidelines of the American Society for Bone and Mineral Research (ASBMR) [35]. For bone histomorphometry, the mice were double-labeled with intra-peritoneal injections of 16 mg/kg of calcein (Sigma) at 5 and 2 days before sacrifice. Lumbar vertebral bodies were removed from each mouse and fixed with 4% PFA in PBS overnight. Lumbar vertebrae were embedded with MMA after dehydration and the plastic sections were cut by a standard microtome (LEICA) into 7 μm for von Kossa staining and 4 μm for TRAP and Toluidine-blue staining. The region of interest was the secondary spongiosa of L3 and L4. Sections were used for analyses when the bases of the bilateral transverse processes were opened. The region of interest (ROI) in the lumbar vertebral body is the secondary spongiosa, which is separated from the primary spongiosa, cranial and caudal growth plate, according to the same protocol as previously performed [8,36]. Histomorphometric analyses were performed using OsteoMeasure (OsteoMetrics, Inc., GA, USA) according to the ASBMR guideline [37].

Isolation of Dmp1-GFP positive osteocytes by FACS

A highly purified population of osteocytes was isolated from neonatal calvariae by FACS using a modified version of the protocol of Paic F et al. [38]. Cells were isolated from 10-day-old fetal mice calvariae of $ER\alpha^{\Delta Ocy/\Delta Ocy}$ and $ER\alpha^{flox/flox}$ also expressing *Dmp1-GFP*. After removal of the sutures, pooled calvarial tissue was subjected to six sequential, 30-minute digestions in a mixture containing 0.05%/0.2 mM trypsin/EDTA and 1.5 U/ml collagenase-P (Roche) at 37 °C. Cell fractions 4 to 6 were collected, pooled, and re-suspended in Dulbecco's modified Eagle's medium (DMEM, Life Technologies) containing 10% FBS (Hyclone) and centrifuged. Cells were rinsed with PBS and re-suspended in PBS/2% FBS and filtered through a 70-μm filter. Cell sorting was performed using a BD FACS Aria cell sorter. The gate for collecting GFP+ cells was set as GFP+ population to represent 10% to 15% of the total cells in GFP+ mice and 0.8% to 1.0% of total cells in GFP− mice (negative control). GFP+ cells were collected in a tube with 500 μl of PBS/3% FBS.

Gene expression microarray

Gene expression microarray was generated using total RNA extracted from the isolated GFP+ osteocytes of $ER\alpha^{\Delta Ocy/\Delta Ocy}$ and $ER\alpha^{flox/flox}$ as previously described [8] and RNA samples were evaluated using the Affymetrix Mouse Genome 430 2.0 Array following standard Affymetrix protocols (GEO: GSE41997). Gene ontology analyses were performed using DAVID Bioinformatics Resources 6.7 [39].

RNA extraction and RT-qPCR

Total RNA from the pulverized femurs or sorted cells was extracted using TRIZOL (Invitrogen) and RNeasy purification kit (QIAGEN). First-strand cDNA was synthesized from total RNA using PrimeScript RT Master Mix (TaKaRa) and subjected to RT-qPCR using SYBR Premix Ex Taq II

(TaKaRa) or KAPA SYBR Fast qPCR Kits (KAPA Biosystems) with Thermal Cycler Dice (TaKaRa) according to the manufacturer's instructions. Primers were purchased from Takara Bio Inc. (Otsu, Japan) or Operon Biotechnologies (Tokyo, Japan) [8]. Gene expression levels were normalized by *Gapdh* or *Rplp0*. Primer sequences were as follow; *Rplp0*: F 5′-TTCCAGGCTTTGGGCATCA-3′ and R 5′-ATGTTCAGCATGTTCAGCAG TGTG-3′, *Gapdh*: F 5′-AAATGGTGAAGGTCGGTGTG-3′ and R 5′-TGAA GGGGTCGTTGATGG-3′, *ERα*: F 5′-CATGGTCATGGTAAGTGGCA-3′ and R 5′-TCTCTGGGCGACATTCTTCT-3′, *Dmp1*: F 5′-TGAAGAGAGGACGGGT GATT-3′ and R 5′-TCCGTGTGGTCACTATTTGC-3′, *Kera*: F 5′-TGGGATGT CCACGACGACTT-3′ and R 5′-AAGGCAGTAGGGAAACTGGGA-3′, *Mdk*: F 5′-TGGAGCCGACTGCAAATACAA-3′ and R 5′-GGCTTAGTCACGCGGA TGG-3′, *Sostdc1*: F 5′-AAATGTATTTGGTGGACCGC-3′ and R 5′-GAATCA AGCCAGGAATGGAG-3′.

Tail suspension

Tail suspension experiments were performed for female $ERα^{ΔOcy/ΔOcy}$ and $ERα^{flox/flox}$ mice for 4 weeks starting at 8 weeks of age according to previous reports [40,41]. Briefly, a stainless steel harness was superglued to the sides of the tail. Female $ERα^{ΔOcy/ΔOcy}$ and $ERα^{flox/flox}$ mice were then suspended from an eye bolt which was secured into the bars of the top of the rat cage. The animal could rotate 360° with the fish swivel and could also move backwards and forwards about 7.5 cm. Water was provided through a standard water bottle with an extra long angled sipper tube to allow the animals to reach the water. Control female $ERα^{ΔOcy/ΔOcy}$ and $ERα^{flox/flox}$ mice were chained to the cage top during the same period of time, but were allowed to load their hindlimbs to minimize the difference in stress-related effects between the tail-suspended groups and the control groups (n = 6 per group).

Statistical analysis

Data were analyzed by a two-tailed student's *t*-test or one-way analysis of variance (ANOVA) to initially determine whether an overall statistically significant change existed before using Tukey's *post hoc* test. For all graphs, data are represented as mean ± SEM. A *p*-value less than 0.05 was considered statistically significant.

Results

Generation of osteocytic ERα deletion mice

To investigate the function of ERα in osteocytes, we generated mice lacking ERα in late-osteoblasts/osteocytes by crossing ERα floxed mice with Dmp1-Cre mice, which express Cre recombinase driven by the Dmp1 promoter. The mice harboring the genotypes of $Dmp1^{Cre}$; $ERα^{L2/L2}$ and $ERα^{L2/L2}$ were analyzed as $ERα^{ΔOcy/ΔOcy}$ and $ERα^{flox/flox}$, respectively. First, to assess cell type specificity of the deletion of the ERα gene locus by Dmp1 promoter-driven Cre recombinase, genomic PCR was performed using DNA extracted from $ERα^{ΔOcy/ΔOcy}$. As a result, a relatively specific deletion of ERα in osteocytes, which were isolated by sequential enzymatic digestion, was detected as an L-band, which was seen only in osteocytes and not in primary cultured osteoblasts or osteoclasts (Fig. 1A). In addition, the ERα mRNA level was examined by qPCR using RNA extracted from femoral bones and GFP-mediated FACS sorted osteocytes of $ERα^{ΔOcy/ΔOcy}$ and $ERα^{flox/flox}$ mice. As a result, there was an approximately 30% and 90% reduction of ERα expression in whole bone and osteocytes, respectively, in $ERα^{ΔOcy/ΔOcy}$ compared to $ERα^{flox/flox}$ mice (Fig. 1B). This significant but low percent deletion in whole bone might reflect ERα expression by other cell types, which are present in the intact femur even though the bone marrow was removed. Also, one group reported that clear deletion of the target gene was detected at the genome level but not the mRNA level when using the Dmp1-Cre mice [42]. Next, body weight was measured every other week from 3 to 12 weeks old. There was no significant difference in body weight between $ERα^{ΔOcy/ΔOcy}$ and $ERα^{flox/flox}$, whereas it was previously reported that ERα total KO mice exhibited a significant increase in body weight [43] (Fig. 1C). Next, we asked if these mice could be a suitable model for analyzing ERα function without the systemic influence of hormones (endocrine disturbances) as described in the conventional ERα null mouse, by examining the concentration of sex steroid hormones. Serum estradiol, testosterone and luteinizing hormone concentrations were measured by ELISA, showing that there were no significant differences between the 12-week-old $ERα^{ΔOcy/ΔOcy}$ and $ERα^{flox/flox}$, regardless of gender (Fig. 1D). Since $ERα^{ΔOcy/ΔOcy}$ mice exhibited a relatively specific deletion of ERα in osteocytes and normal serum sex steroid hormone levels, we concluded that $ERα^{ΔOcy/ΔOcy}$ could be used for analysis of ERα function in osteocytes without the complications of endocrine disturbances.

Osteocytic ERα deletion female mice exhibit an osteopenic phenotype

The BMD of 12-week-old $ERα^{ΔOcy/ΔOcy}$ and $ERα^{flox/flox}$ were measured by DXA, showing that the BMD of female $ERα^{ΔOcy/ΔOcy}$ was significantly decreased in the proximal, not in middle and distal, tibiae compared to that of female $ERα^{flox/flox}$ (Fig. 1E). However, the BMD of tibiae from male $ERα^{ΔOcy/ΔOcy}$ were not significantly different from that of male $ERα^{flox/flox}$ (Fig. 1E). Next, to assess changes in bone structure between female $ERα^{ΔOcy/ΔOcy}$ and $ERα^{flox/flox}$ mice, μCT analysis was performed. Decreased trabecular bone mass in $ERα^{ΔOcy/ΔOcy}$ mice was observed by μCT analysis (Fig. 2A). Trabecular bone of female $ERα^{ΔOcy/ΔOcy}$ exhibited a significant decrease in BV/TV, vBMD, Tb.N and Conn-D, and an increase in Tb.Sp and SMI compared to those of female $ERα^{flox/flox}$ (Fig. 2B). The parameters in metaphyseal cortical bone of female $ERα^{ΔOcy/ΔOcy}$ were not significantly different from that of female $ERα^{flox/flox}$ (Fig. 2C).

Osteocytic ERα regulates bone formation through control of osteoblasts

To examine whether the reduced bone phenotype of $ERα^{ΔOcy/ΔOcy}$ could be caused by alterations in the potential interaction between osteocytes and either osteoblasts or osteoclasts, bone histomorphometry was performed. The number and/or activity of osteoblasts/osteoclasts were examined in $ERα^{ΔOcy/ΔOcy}$ and $ERα^{flox/flox}$, using lumbar vertebrae of 12-week-old female $ERα^{ΔOcy/ΔOcy}$ and $ERα^{flox/flox}$. Parameters related to osteoblastic bone formation, such as N.Ob/B.Pm and Ob.S/BS, were significantly decreased in $ERα^{ΔOcy/ΔOcy}$ compared to $ERα^{flox/flox}$ (Fig. 3). In addition, N.Ocy/B.Ar was also decreased in $ERα^{ΔOcy/ΔOcy}$, which might be due to a decreased number of osteoblasts, which are precursors of osteocytes. Also, the reduction of BFR/BS and MAR in $ERα^{ΔOcy/ΔOcy}$ tended to be significant ($p = 0.07$), due to the reduction of osteoblastic parameters. On the other hand, parameters related to osteoclastic bone resorption, such as N.Oc/B.Pm and Oc.S/BS, were not altered in $ERα^{ΔOcy/ΔOcy}$ when compared to $ERα^{flox/flox}$ (Fig. 3). These results suggested that deficiency of ERα in osteocytes could decrease the number of osteoblasts and consequently their bone forming activity, indicating that bone mass reduction in $ERα^{ΔOcy/ΔOcy}$ could be caused by a reduction of osteoblastic bone formation, not a promotion of osteoclastic bone resorption. In addition, this result implies that osteocytic ERα might positively regulate osteoblastic bone formation by signaling from osteocytes, such as in a paracrine manner or by cell–cell contact.

Gene expression profiles of osteocytes lacking ERα

To determine what secretory proteins or signaling pathways *ERα* may utilize in osteocytes, a gene array analysis of Dmp1-GFP-positive cells from controls and mice with a targeted deletion of *ERα* in osteocytes was performed. Dmp1-GFP mice were crossed with $Dmp1^{Tg/0}$; $ERα^{L2/L2}$ mice to generate *Dmp1-GFP+*; $Dmp1^{Tg/0}$; $ERα^{L2/+}$ mice, and then *Dmp1-GFP+*; $Dmp1^{Tg/0}$; $ERα^{L2/L2}$ (*Dmp1-GFP+*; $ERα^{ΔOcy/ΔOcy}$) and

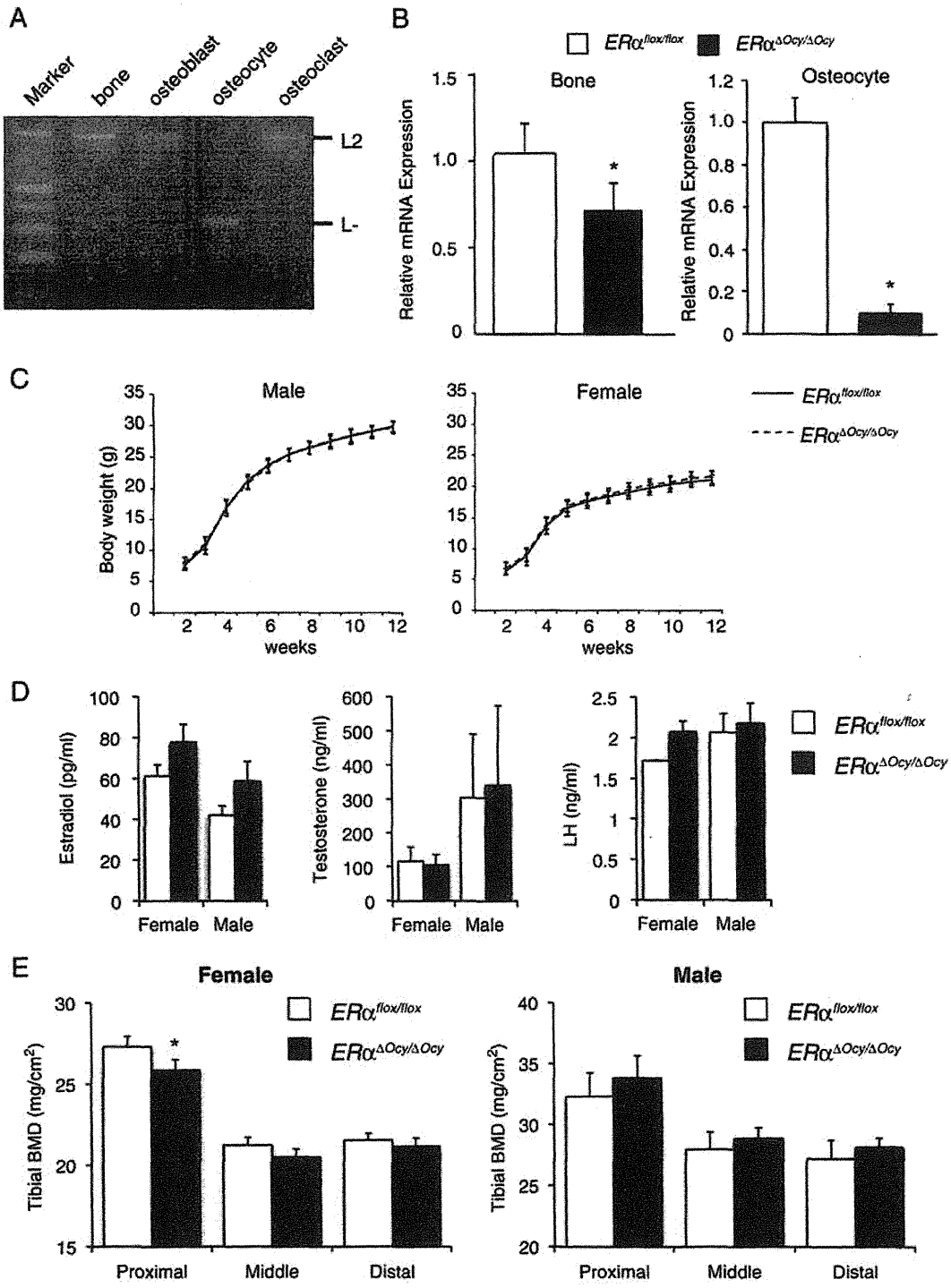

Fig. 1. Generation of mice with targeted deletion of ERα in osteocytes. (A) Deletion of ERα gene locus in osteocyte was detected by genome PCR in $ERα^{ΔOcy/ΔOcy}$. (B) mRNA levels of ERα from whole femurs (left panel) and isolated osteocytes (right panel) of $ERα^{flox/flox}$ and $ERα^{ΔOcy/ΔOcy}$ mice was evaluated by RT-qPCR. Data are represented as mean ± SEM (n = 3). (C) The growth curves of $ERα^{flox/flox}$ and $ERα^{ΔOcy/ΔOcy}$ mice. Data are represented as mean ± SEM (n = 7–10). (D) Serum hormone levels of 12-week-old $ERα^{flox/flox}$ and $ERα^{ΔOcy/ΔOcy}$ mice. Data are represented as mean ± SEM (n = 4–7). (E) BMD of 1/3 portion of longitudinal divisions of tibiae from 12-week-old $ERα^{flox/flox}$ and $ERα^{ΔOcy/ΔOcy}$ mice. Data are represented as mean ± SEM (Female n = 8, Male n = 7). * indicates $p < 0.05$.

Dmp1-GFP+; $ERα^{L2/L2}$ (*Dmp1-GFP+*; $ERα^{flox/flox}$) were generated by crossing *Dmp1-GFP+*; $Dmp1^{Tg/0}$; $ERα^{L2/+}$ and $ERα^{L2/L2}$. Calvariae obtained from approximately 10-day-old female *Dmp1-GFP+*; $ERα^{ΔOcy/ΔOcy}$ and *Dmp1-GFP+*; $ERα^{flox/flox}$ were treated with sequential enzymatic digestion and subjected to FACS. The percentage of GFP + cells in fractions 4 to 6 was increased compared to that in fractions 2 to 4 (23.3% and 8.2%, respectively) (Fig. 4A). To determine if osteocytes were highly purified in this system, gene expression of cell-type specific marker genes in GFP + cells (osteocytes) and GFP − cells (osteoblasts) was confirmed by RT-qPCR. As a result, the expression of Dmp1 (osteocyte marker

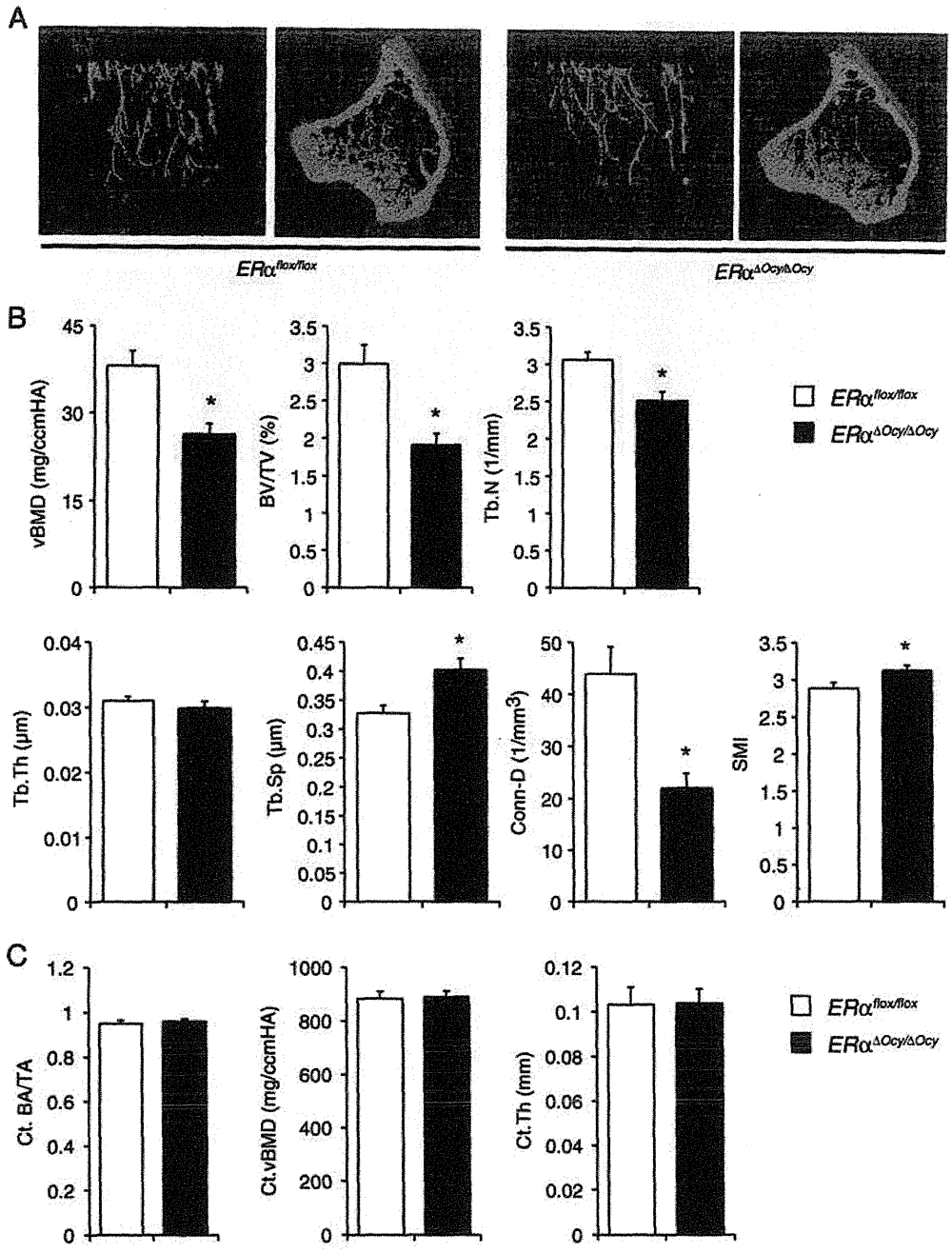

Fig. 2. μCT analyses of the mice lacking ERα in osteocytes. (A) Representative μCT views. (B) 3D measurements of proximal tibiae from $ERα^{flox/flox}$ and $ERα^{ΔOcy/ΔOcy}$ mice. Data are represented as mean ± SEM (n = 10). * indicates $p < 0.05$.

gene) in GFP+ cells was about 25 times higher than in GFP− cells, while the expression of keratocan, Kera, (osteoblast marker gene) in GFP− cells was about 25 times higher than in GFP+ cells (Fig. 4B). Extracted total RNA from *Dmp1-GFP+*; $ERα^{ΔOcy/ΔOcy}$ (n = 3) and *Dmp1-GFP+*; $ERα^{flox/flox}$ (n = 3) was subjected to a gene expression microarray analysis with GeneChip Mouse Genome 430 2.0 (Affymetrix). There were 276 genes found to be significantly differentially expressed between $ERα^{ΔOcy/ΔOcy}$ and $ERα^{flox/flox}$ ($p < 0.01$). Among them, 76 genes were significantly down-regulated and 200 genes were up-regulated (Fig. 4C). Gene ontology analyses revealed that 'secreted' was listed top in the Keyword analysis when sorted by *p*-value (Fig. 4D). Among these genes, *Mdk* (Midkine) and *Sostdc1* (Sclerostin domain containing 1) were significantly up-regulated in $ERα^{ΔOcy/ΔOcy}$ although there were no significant differences in *Sost* or β-catenin (*Ctnnb1*) gene expression (Fig. 4E). Up-regulation of mRNA of *Mdk* and *Sostdc1* in $ERα^{ΔOcy/ΔOcy}$ was also validated when determined by RT-qPCR (Fig. 4F). From the results of functional annotation in differentially expressed genes between $ERα^{ΔOcy/ΔOcy}$ and $ERα^{flox/flox}$, osteocytic ERα could regulate the expression of secretory protein genes such as *Mdk* and *Sostdc1*, which have been shown to be inhibitors of Wnt signaling-related bone formation [44–46]. However, the expression levels of *Mdk* and *Sostdc1* were not significantly altered when late-stage primary cultured osteoblasts

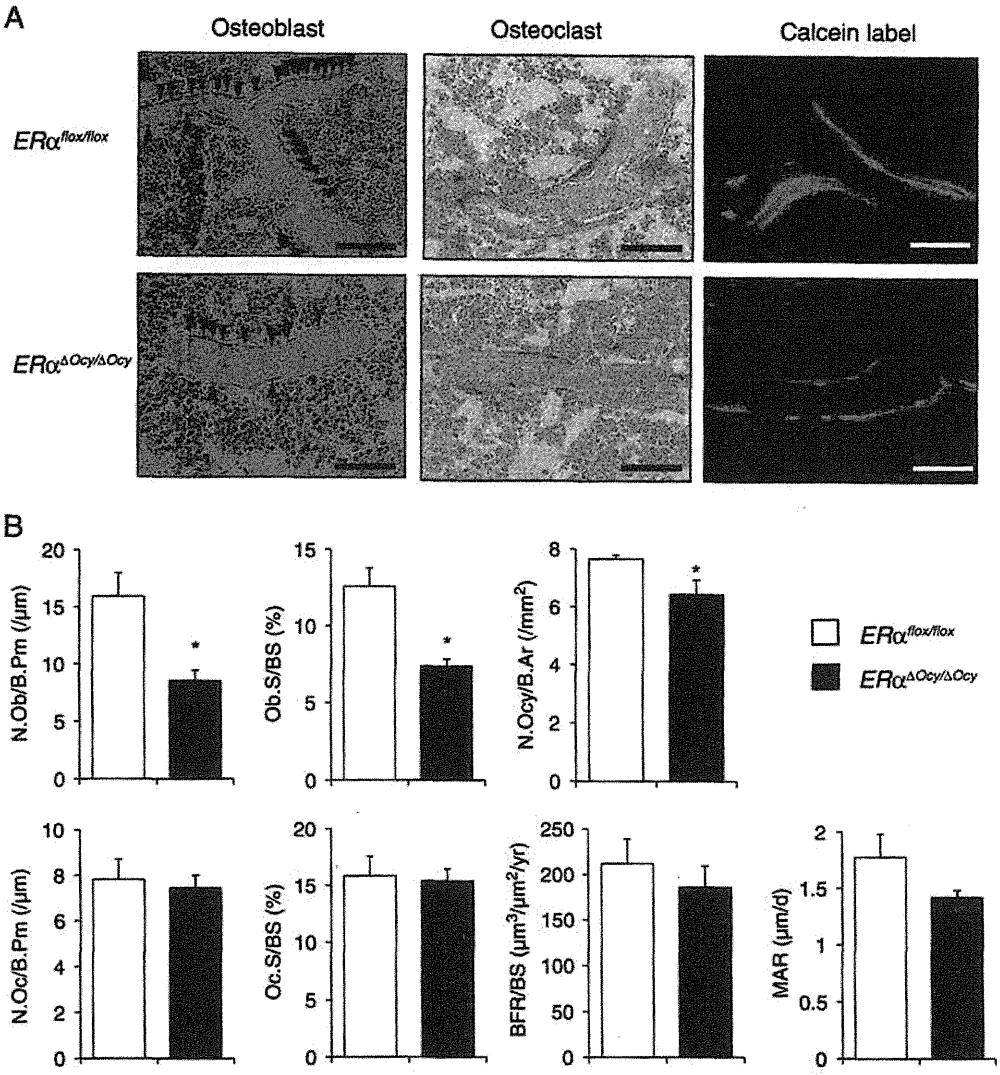

Fig. 3. $ER\alpha^{\Delta Ocy/\Delta Ocy}$ mice exhibit decreased bone formation. (A) Representative views of Toluidine blue staining for mononuclear cuboidal osteoblasts (arrowhead), TRAP staining for multinuclear TRAP-positive osteoclasts and calcein labeling for dynamic parameters are shown. Bars indicate 50 μm. (B) Data are represented as mean ± SEM (n = 6). * indicates $p < 0.05$.

were treated with 17β-estradiol for 2 or 6 h (Supplemental Fig. S1), indicating that *Mdk* and *Sostdc1* might not be early responsive genes, but be indirect target genes.

Trabecular bone loss is exacerbated in $ER\alpha^{\Delta Ocy/\Delta Ocy}$ in response to unloading while cortical bone is resistant to unloading-induced bone loss

ERα has been reported to be involved in mechanosensing and increasing cortical bone formation under overloading conditions [11]. The hindlimb tail suspension model is a well-known model for unloading (or immobilization) and it is also reported that tail suspension-induced bone loss is significantly enhanced by ovariectomy [47]. To determine whether osteocytic ERα plays any roles in unloading-induced bone loss, a hindlimb suspension experiment was performed for female $ER\alpha^{\Delta Ocy/\Delta Ocy}$ and $ER\alpha^{flox/flox}$ for 4 weeks starting at 8 weeks of age. Control mice were chained to the cage top during the same period but allowed to load their hindlimbs to control for stress related effects.

During the 4-week experimental period, the average body weight of the experimental group increased 1 g, whereas the control group increased 2 g (Supplemental Fig. S2). Although there was a significant difference in body weight increase over the four weeks between the experimental and control groups, there was no significant difference in body weight between $ER\alpha^{\Delta Ocy/\Delta Ocy}$ and $ER\alpha^{flox/flox}$ within each group at the end of the experiment (Supplemental Fig. S2). Femoral diaphysis and distal metaphysis of the unloaded and loaded groups of both genotypes ($ER\alpha^{\Delta Ocy/\Delta Ocy}$ and $ER\alpha^{flox/flox}$) were measured using μCT. vBMD in the femoral diaphysis of tail suspended female $ER\alpha^{\Delta Ocy/\Delta Ocy}$ was significantly higher than that of $ER\alpha^{flox/flox}$ (Figs. 5A and B), although there were no significant differences in bone area or cortical thickness between genotypes. Upon further analysis, it was found that the trabecular bone mass was decreased in unloaded mice regardless of genotypes, and tail suspension induced trabecular bone loss in $ER\alpha^{\Delta Ocy/\Delta Ocy}$ was greater than that in $ER\alpha^{flox/flox}$ (Figs. 5C and D). These data indicate that osteocytic ERα is protective against trabecular bone loss due to unloading.

Discussion

Based on reports on the functions of ERα in bone, estrogens are osteoprotective by regulating the life span of osteoclasts through osteoclastic and osteoblastic ERα and also by inhibiting apoptosis of osteoblasts and osteocytes [8,9,48–50]. Recently, it was reported that osteoblastic ERα has an osteoprotective function [12,14,15], however, little is known about the role of osteocytes in the osteoprotective actions

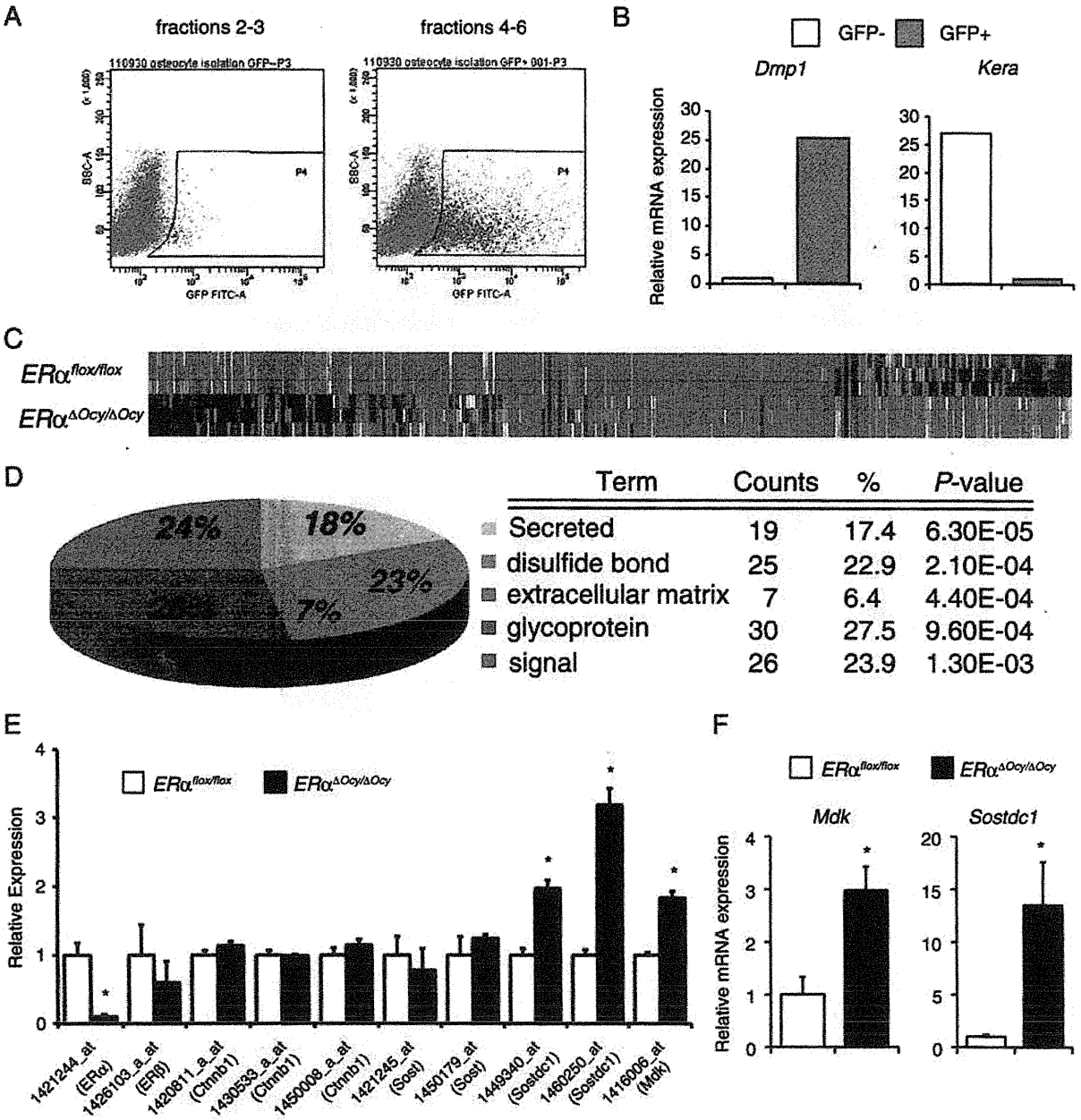

Fig. 4. Osteocytes lacking ERα show increased Mdk and Sostdc1 expression. (A) Two-dimensional dot plot of cells obtained from sequential enzymatic digestion of calvariae of mice expressing Dmp1-GFP. Left: fractions 2–3, right: fractions 4–6. (B) Expression of osteocyte (Dmp1) and osteoblast (Kera) marker genes in the GFP− and GFP+ population of isolated cells. (C) Heat map of significantly regulated genes in the gene expression microarray using total RNA from isolated GFP+ cells of $ERα^{flox/flox}$ and $ERα^{ΔOcy/ΔOcy}$ mice harboring Dmp1-GFP (n = 3). Red: high expression. Blue: low expression. (D) Functional annotation clustering of Keywords by DAVID Bioinformatic Resources. (E) Relative microarray intensity of each probe for ERα, ERβ, Ctnnb1 (β-catenin), Sost, Sostdc1 and Mdk. Data are represented as mean ± SEM (n = 3). (F) RT-qPCR for Mdk and Sostdc1 as same as panel E. * indicates $p < 0.05$.

of estrogens in skeletal homeostasis. To decipher the direct functions of ERα in osteocytes, the most abundant bone cell type in the adult skeleton, mice lacking ERα in osteocytes were genetically generated and their bone phenotype were analyzed in this study. ERα in osteocytes was found to play a significant role in maintaining bone mass by regulating osteoblastic bone formation only in females. It was further revealed that ERα in osteocytes is supportive for maintaining trabecular bone mass not only under normal loading conditions but also under tail suspension-induced unloading, which can be considered as experimental recapitulation of immobilization or space flight. However, the absence of this receptor protected against cortical bone loss. These results are consistent with a previous report in which bone mass adaptation induced by mechanical loading was impaired in ERα null mice [11]. Together, these results indicate that osteocyte mechanosensations at least in part *via* osteocytic ERα.

Maatta et al. and Melville et al. suggested that ERα in mature osteoblasts plays a role in maintaining trabecular bone mass in females based on analyses of mice lacking ERα in mature osteoblasts using Osteocalcin-Cre mice [12,15]. Almeida et al. suggested that ERα in osteoblast progenitors, but not in mature osteoblasts or osteocytes, is essential for regulation of female cortical bone [14]. As mentioned above, the functions of ERα in osteoblast lineage cells *in vivo* are still controversial and it is important to combine knowledge from various studies. All female mice exhibited an osteopenic phenotype in both the osteoblast-specific ERα

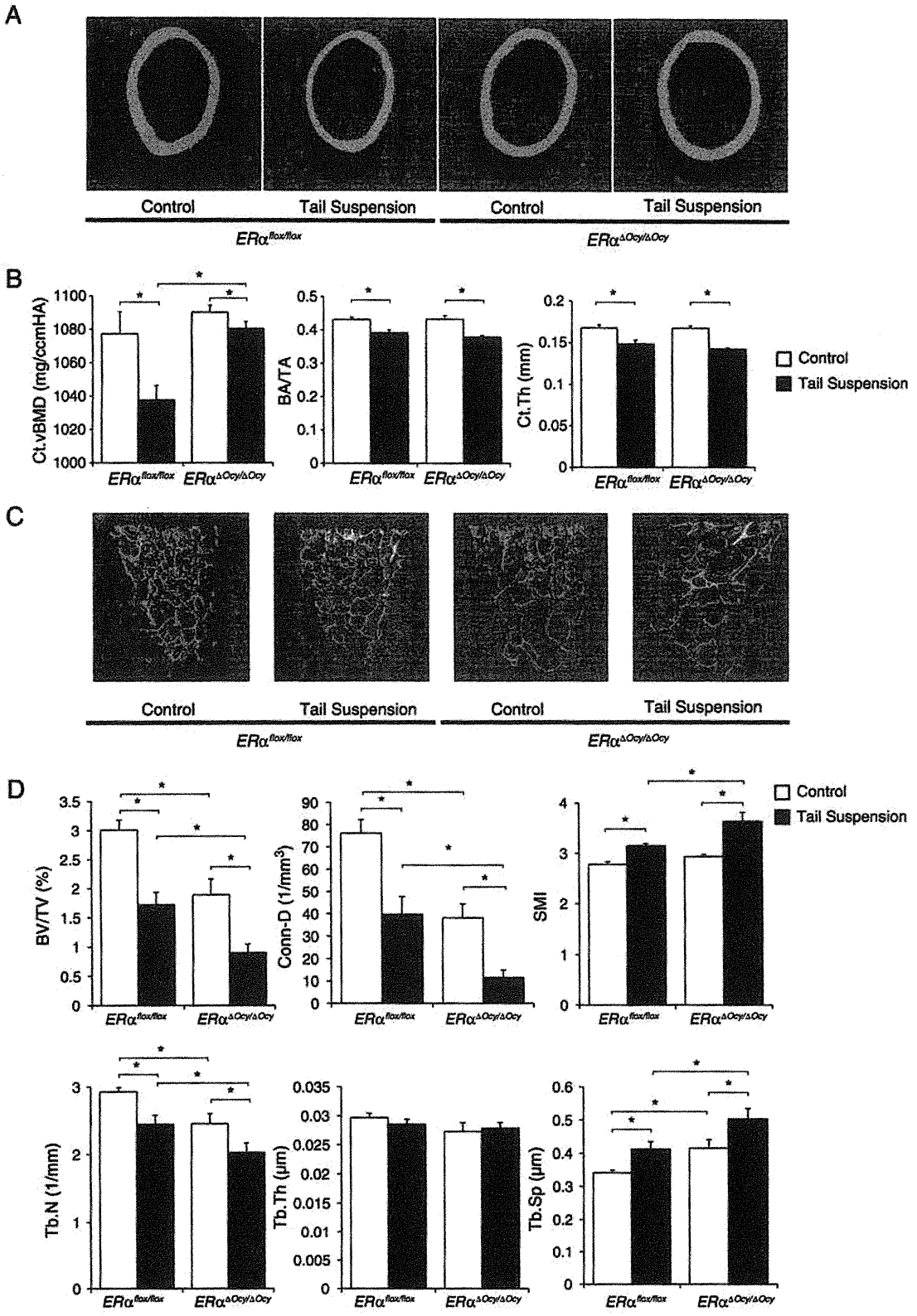

Fig. 5. Effects of unloading on trabecular and cortical bone in mice with targeted deletion of ERα in osteocytes. (A and C) Representative μCT views. (B) 3D measurements of femoral distal trabecular area and (D) 3D measurements of femoral diaphyses from $ERα^{flox/flox}$ and $ERα^{ΔOcy/ΔOcy}$ mice subjected or not subjected to tail suspension. Data are represented as mean ± SEM ($n = 6$). * indicates $p < 0.05$.

knockout mice by Maatta et al. and Almeida et al., and in previous reports regarding osteoclast-specific ERα knockout mice [8,9]. As would be predicted, androgen receptor knockout mice (ARKO), including both systemic ARKO [51] and osteocyte conditional ARKO [52], exhibited bone loss in male mice. These gender-specific phenotypes are probably caused by differences in concentration of circulating sex steroids, estrogens and androgens. In contrast to these studies and our present study, a recent report showed that mice lacking ERα using the same Dmp1-Cre mouse exhibited trabecular bone loss only in male mice, but not in female mice [13]. In this report, Windahl et al. proposed that the physiological trabecular bone-sparing effect of estrogen is mediated *via* ERα in osteocytes in males, but also *via* ERα in osteoclasts in females [13]. At present, it is difficult to provide a convincing explanation to describe the discrepancies between our current study and this report [13]. However, one possible reason may be differences in the genetic background of the mouse strain of the ERα-floxed mice since the Dmp1-Cre mice were identical. The ERα-floxed mice used in our study have been registered as *Esr1*^{tm1Mma} and originated from 129S2/SvPas mixed background, and published in 2000 [5], then backcrossed with C57BL6 line for more than 10 times. On the other hand, the ERα-floxed mice used in the study by Windahl et al. have been registered as *Esr1*^{tm1Gust} and originated from 129X1/SvJ mixed background, and published in 2012 [53]. These differences might be responsible for the discrepancies between the two studies. Regardless, the results of these two studies suggest that osteocytic ERα may have a role in maintenance of trabecular bone homeostasis regardless of gender.

To investigate the possible molecular basis underlying ERα function in osteocytes, we performed an osteocyte isolation technique using FACS analysis of Dmp1-GFP positive cells from conditional null mice and their controls. The results obtained from the Functional Annotation Clustering of differentially expressed genes suggested that osteocytic ERα might regulate transcription of the genes related to secretory proteins, which may regulate osteoblastic bone formation and contribute to maintenance of bone homeostasis. In fact, Sostdc1, an antagonist of the Wnt signaling [45,54], was elevated as a downstream gene of osteocytic ERα. Sostdc1 is a gene also called Wise or Ectodin whose domain is similar to Sost (Sclerostin). Sost and Sostdc1 bind to Wnt co-receptors called Lrps and regulate the Wnt/β-catenin pathway negatively [55]. Wnt signal proteins are reported to modulate bone mass *in vivo* by acting directly on mesenchymal stem cells [56–59]. Genes involved in the Wnt signaling are known to regulate the cell proliferation, differentiation, and apoptosis of osteoblasts [60]. Interaction between β-catenin and ERα has been previously reported [61] and the expressions of some Wnt family genes are important for responding to mechanical stress and are reportedly regulated by ERα [32]. Conventional Sostdc1 KO mice are reported to exhibit abnormal tooth development, which has similar characteristics as bone [45,54]. Also, it has been reported that estradiol regulates mRNA levels of Sostdc1 in U2OS cells [62]. In addition, a meta-analysis of BMD in a female Chinese population revealed that a mutation in the Sostdc1 cording region was correlated with BMD, suggesting that Sostdc1 might play a role in homeostasis of bone metabolism [46].

Also, Midkine, Mdk, was elevated as a downstream molecule of ERα in mice with this targeted deletion. Mdk is a member of a family of heparin-binding growth factors known primarily for their effects on neural cells [63]. Mdk expression is reported to increase during the course of primary osteoblast differentiation. Mdk has been shown to bind to a complex of protein tyrosine phosphatase zeta (Ptprx), low-density lipoprotein receptor-related protein-6 (Lrp6), and exert negative effects on Wnt signaling [64]. Conventional Mdk null mice exhibit increased bone formation, suggesting Mdk is a negative regulator of osteoblastic bone formation. Furthermore, Mdk KO mice are resistant to OVX-induced bone loss and sensitive to mechanical loading induced cortical bone increase [44]. In addition, the expression of ALP and the induction of canonical Wnt signaling in MC3T3E1, an osteoblastic cell line, were inhibited by Mdk treatments [64]. These reports and the results from our current study suggest that Sostdc1 and Mdk might be responsible for a component of estrogen's osteoprotective actions.

However, questions remain regarding how ERα negatively regulates the transcription of these genes because there are no reports of a negative transcriptional regulation of the estrogen receptor response element (negative ERE), although details of a negative glucocorticoid receptor response element (nGRE) have been reported [65]. Alternatively, it is possible that the expression of these factors might be regulated by an ERα-dependent miRNA. The precise molecular basis of transcriptional regulation or mRNA stabilization of these genes must be clarified in future studies. Neutralizing or deletion studies of these two proteins in this mouse model could provide possible answers for these questions.

In conclusion, osteocytic ERα might play a role in estrogen's osteoprotective action by controlling the expression of Wnt antagonists, which regulate osteoblastic bone formation in trabecular bone.

Supplementary data to this article can be found online at http://dx.doi.org/10.1016/j.bone.2013.12.005.

Conflict of interest

All authors state that they have no conflicts of interest.

Acknowledgments

The authors thank Dr. S. Kato for his general support and discussion, Ms. Noriko Moriyama for her technical support (microarray). This work was supported by Grant-in-Aids from Japan Society for the Promotion of Science (Research fellowship for young scientist to SK), NIH NIAMS PO1 AR046798 (to LFB) and JSPS KAKENHI (Grant numbers 23689066 and 23659712 to YI).

References

[1] Nelson HD. Menopause. Lancet 2008;371:760–70.
[2] Imai Y, Kondoh S, Kouzmenko A, Kato S. Minireview: osteoprotective action of estrogens is mediated by osteoclastic estrogen receptor-alpha. Mol Endocrinol 2010;24:877–85.
[3] Sun L, Peng Y, Sharrow AC, Iqbal J, Zhang Z, Papachristou DJ, et al. FSH directly regulates bone mass. Cell 2006;125:247–60.
[4] Pacifici R. Estrogen deficiency, T cells and bone loss. Cell Immunol 2008;252:68–80.
[5] Dupont S, Krust A, Gansmuller A, Dierich A, Chambon P, Mark M. Effect of single and compound knockouts of estrogen receptors alpha (ERalpha) and beta (ERbeta) on mouse reproductive phenotypes. Development 2000;127:4277–91.
[6] Windahl SH, Andersson G, Gustafsson JA. Elucidation of estrogen receptor function in bone with the use of mouse models. Trends Endocrinol Metab 2002;13:195–200.
[7] Sims NA, Dupont S, Krust A, Clement-Lacroix P, Minet D, Resche-Rigon M, et al. Deletion of estrogen receptors reveals a regulatory role for estrogen receptors-beta in bone remodeling in females but not in males. Bone 2002;30:18–25.
[8] Nakamura T, Imai Y, Matsumoto T, Sato S, Takeuchi K, Igarashi K, et al. Estrogen prevents bone loss *via* estrogen receptor alpha and induction of Fas ligand in osteoclasts. Cell 2007;130:811–23.
[9] Martin-Millan M, Almeida M, Ambrogini E, Han L, Zhao H, Weinstein RS, et al. The estrogen receptor-alpha in osteoclasts mediates the protective effects of estrogens on cancellous but not cortical bone. Mol Endocrinol 2010;24:323–34.
[10] Tomkinson A, Reeve J, Shaw RW, Noble BS. The death of osteocytes *via* apoptosis accompanies estrogen withdrawal in human bone. J Clin Endocrinol Metab 1997;82:3128–35.
[11] Lee K, Jessop H, Suswillo R, Zaman G, Lanyon L. Endocrinology: bone adaptation requires oestrogen receptor-alpha. Nature 2003;424:389.
[12] Maatta JA, Buki KG, Gu G, Alanne MH, Vaaraniemi J, Liljenback H, et al. Inactivation of estrogen receptor alpha in bone-forming cells induces bone loss in female mice. FASEB J 2012;27:478–88.
[13] Windahl SH, Borjesson AE, Farman HH, Engdahl C, Moverare-Skrtic S, Sjogren K, et al. Estrogen receptor-alpha in osteocytes is important for trabecular bone formation in male mice. Proc Natl Acad Sci U S A 2013;110:2294–9.
[14] Almeida M, Iyer S, Martin-Millan M, Bartell SM, Han L, Ambrogini E, et al. Estrogen receptor-alpha signaling in osteoblast progenitors stimulates cortical bone accrual. J Clin Invest 2013;123:394–404.
[15] Melville KM, Kelly NH, Khan SA, Schimenti JC, Ross FP, Main RP, et al. Female mice lacking estrogen receptor-alpha in osteoblasts have compromised bone mass and strength. J Bone Miner Res 2013 (in press) (Epub ahead of print).
[16] Burger EH, Klein-Nulend J. Mechanotransduction in bone–role of the lacuno-canalicular network. FASEB J 1999(13 Suppl.):S101–12.

[17] Robling AG, Niziolek PJ, Baldridge LA, Condon KW, Allen MR, Alam I, et al. Mechanical stimulation of bone in vivo reduces osteocyte expression of Sost/sclerostin. J Biol Chem 2008;283:5866–75.
[18] Skerry TM, Bitensky L, Chayen J, Lanyon LE. Early strain-related changes in enzyme activity in osteocytes following bone loading in vivo. J Bone Miner Res 1989;4:783–8.
[19] Gluhak-Heinrich J, Ye L, Bonewald LF, Feng JQ, MacDougall M, Harris SE, et al. Mechanical loading stimulates dentin matrix protein 1 (DMP1) expression in osteocytes in vivo. J Bone Miner Res 2003;18:807–17.
[20] Gluhak-Heinrich J, Pavlin D, Yang W, MacDougall M, Harris SE. MEPE expression in osteocytes during orthodontic tooth movement. Arch Oral Biol 2007;52:684–90.
[21] Thompson DL, Sabbagh Y, Tenenhouse HS, Roche PC, Drezner MK, Salisbury JL, et al. Ontogeny of Phex/PHEX protein expression in mouse embryo and subcellular localization in osteoblasts. J Bone Miner Res 2002;17:311–20.
[22] Nampei A, Hashimoto J, Hayashida K, Tsuboi H, Shi K, Tsuji I, et al. Matrix extracellular phosphoglycoprotein (MEPE) is highly expressed in osteocytes in human bone. J Bone Miner Metab 2004;22:176–84.
[23] Liu S, Zhou J, Tang W, Jiang X, Rowe DW, Quarles LD. Pathogenic role of Fgf23 in Hyp mice. Am J Physiol Endocrinol Metab 2006;291:E38–49.
[24] Feng JQ, Ward LM, Liu S, Lu Y, Xie Y, Yuan B, et al. Loss of DMP1 causes rickets and osteomalacia and identifies a role for osteocytes in mineral metabolism. Nat Genet 2006;38:1310–5.
[25] Bonewald LF. Osteocytes as dynamic multifunctional cells. Ann N Y Acad Sci 2007;1116:281–90.
[26] Bergmann P, Body JJ, Boonen S, Boutsen Y, Devogelaer JP, Goemaere S, et al. Loading and skeletal development and maintenance. J Osteoporos 2010;2011:786752.
[27] Lloyd SA, Bandstra ER, Willey JS, Riffle SE, Tirado-Lee L, Nelson GA, et al. Effect of proton irradiation followed by hindlimb unloading on bone in mature mice: a model of long-duration spaceflight. Bone 2012;51:756–64.
[28] Lee KC, Maxwell A, Lanyon LE. Validation of a technique for studying functional adaptation of the mouse ulna in response to mechanical loading. Bone 2002;31:407–12.
[29] Bonewald LF, Johnson ML. Osteocytes, mechanosensing and Wnt signaling. Bone 2008;42:606–15.
[30] Robinson JA, Chatterjee-Kishore M, Yaworsky PJ, Cullen DM, Zhao W, Li C, et al. Wnt/beta-catenin signaling is a normal physiological response to mechanical loading in bone. J Biol Chem 2006;281:31720–8.
[31] Javaheri B, Stern A, Lara N, Dallas M, Zhao H, Liu Y, et al. Deletion of a single beta-catenin allele in osteocytes abolishes the bone anabolic response to loading. J Bone Miner Res 2013 (in press) (Epub ahead of print).
[32] Armstrong VJ, Muzylak M, Sunters A, Zaman G, Saxon LK, Price JS, et al. Wnt/beta-catenin signaling is a component of osteoblastic bone cell early responses to load-bearing and requires estrogen receptor alpha. J Biol Chem 2007;282:20715–27.
[33] Lu Y, Xie Y, Zhang S, Dusevich V, Bonewald LF, Feng JQ. DMP1-targeted Cre expression in odontoblasts and osteocytes. J Dent Res 2007;86:320–5.
[34] Kalajzic I, Braut A, Guo D, Jiang X, Kronenberg MS, Mina M, et al. Dentin matrix protein 1 expression during osteoblastic differentiation, generation of an osteocyte GFP-transgene. Bone 2004;35:74–82.
[35] Bouxsein ML, Boyd SK, Christiansen BA, Guldberg RE, Jepsen KJ, Muller R. Guidelines for assessment of bone microstructure in rodents using micro-computed tomography. J Bone Miner Res 2010;25:1468–86.
[36] Sato S, Hanada R, Kimura A, Abe T, Matsumoto T, Iwasaki M, et al. Central control of bone remodeling by neuromedin U. Nat Med 2007;13:1234–40.
[37] Parfitt AM, Drezner MK, Glorieux FH, Kanis JA, Malluche H, Meunier PJ, et al. Bone histomorphometry: standardization of nomenclature, symbols, and units. Report of the ASBMR Histomorphometry Nomenclature Committee. J Bone Miner Res 1987;2:595–610.
[38] Paic F, Igwe JC, Nori R, Kronenberg MS, Franceschetti T, Harrington P, et al. Identification of differentially expressed genes between osteoblasts and osteocytes. Bone 2009;45:682–92.
[39] Huang da W, Sherman BT, Lempicki RA. Systematic and integrative analysis of large gene lists using DAVID bioinformatics resources. Nat Protoc 2009;4:44–57.
[40] McCarthy JJ, Fox AM, Tsika GL, Gao L, Tsika RW. Beta-MHC transgene expression in suspended and mechanically overloaded/suspended soleus muscle of transgenic mice. Am J Physiol 1997;272:R1552–61.
[41] Tsika G, Ji J, Tsika R. Sp3 proteins negatively regulate beta myosin heavy chain gene expression during skeletal muscle inactivity. Mol Cell Biol 2004;24:10777–91.
[42] Xiong J, Onal M, Jilka RL, Weinstein RS, Manolagas SC, O'Brien CA. Matrix-embedded cells control osteoclast formation. Nat Med 2011;17:1235–41.
[43] Heine PA, Taylor JA, Iwamoto GA, Lubahn DB, Cooke PS. Increased adipose tissue in male and female estrogen receptor-alpha knockout mice. Proc Natl Acad Sci U S A 2000;97:12729–34.
[44] Neunaber C, Catala-Lehnen P, Beil FT, Marshall RP, Kanbach V, Baranowsky A, et al. Increased trabecular bone formation in mice lacking the growth factor midkine. J Bone Miner Res 2010;25:1724–35.
[45] Ahn Y, Sanderson BW, Klein OD, Krumlauf R. Inhibition of Wnt signaling by Wise (Sostdc1) and negative feedback from Shh controls tooth number and patterning. Development 2010;137:3221–31.
[46] He JW, Yue H, Hu WW, Hu YQ, Zhang ZL. Contribution of the sclerostin domain-containing protein 1 (SOSTDC1) gene to normal variation of peak bone mineral density in Chinese women and men. J Bone Miner Metab 2011;29:571–81.
[47] Tou JC, Foley A, Yuan YV, Arnaud S, Wade CE, Brown M. The effect of ovariectomy combined with hindlimb unloading and reloading on the long bones of mature Sprague–Dawley rats. Menopause 2008;15:494–502.
[48] Almeida M, Martin-Millan M, Ambrogini E, Bradsher 3rd R, Han L, Chen XD, et al. Estrogens attenuate oxidative stress and the differentiation and apoptosis of osteoblasts by DNA-binding-independent actions of the ERalpha. J Bone Miner Res 2010;25:769–81.
[49] Tomkinson A, Gevers EF, Wit JM, Reeve J, Noble BS. The role of estrogen in the control of rat osteocyte apoptosis. J Bone Miner Res 1998;13:1243–50.
[50] Krum SA, Miranda-Carboni GA, Hauschka PV, Carroll JS, Lane TF, Freedman LP, et al. Estrogen protects bone by inducing Fas ligand in osteoblasts to regulate osteoclast survival. EMBO J 2008;27:535–45.
[51] Kawano H, Sato T, Yamada T, Matsumoto T, Sekine K, Watanabe T, et al. Suppressive function of androgen receptor in bone resorption. Proc Natl Acad Sci U S A 2003;100:9416–21.
[52] Sinnesael M, Claessens F, Laurent M, Dubois V, Boonen S, Deboel L, et al. Androgen receptor (AR) in osteocytes is important for the maintenance of male skeletal integrity: evidence from targeted AR disruption in mouse osteocytes. J Bone Miner Res 2012;27:2535–43.
[53] Antonson P, Omoto Y, Humire P, Gustafsson JA. Generation of ERalpha-floxed and knockout mice using the Cre/LoxP system. Biochem Biophys Res Commun 2012;424:710–6.
[54] Cho SW, Kwak S, Woolley TE, Lee MJ, Kim EJ, Baker RE, et al. Interactions between Shh, Sostdc1 and Wnt signaling and a new feedback loop for spatial patterning of the teeth. Development 2011;138:1807–16.
[55] Itasaki N, Jones CM, Mercurio S, Rowe A, Domingos PM, Smith JC, et al. Wise, a context-dependent activator and inhibitor of Wnt signalling. Development 2003;130:4295–305.
[56] Liu G, Vijayakumar S, Grumolato L, Arroyave R, Qiao H, Akiri G, et al. Canonical Wnts function as potent regulators of osteogenesis by human mesenchymal stem cells. J Cell Biol 2009;185:67–75.
[57] Takada I, Kouzmenko AP, Kato S. Wnt and PPARgamma signaling in osteoblastogenesis and adipogenesis. Nat Rev Rheumatol 2009;5:442–7.
[58] Augello A, De Bari C. The regulation of differentiation in mesenchymal stem cells. Hum Gene Ther 2010;21:1226–38.
[59] Baron R, Kneissel M. WNT signaling in bone homeostasis and disease: from human mutations to treatments. Nat Med 2013;19:179–92.
[60] Westendorf JJ, Kahler RA, Schroeder TM. Wnt signaling in osteoblasts and bone diseases. Gene 2004;341:19–39.
[61] Kouzmenko AP, Takeyama K, Ito S, Furutani T, Sawatsubashi S, Maki A, et al. Wnt/beta-catenin and estrogen signaling converge in vivo. J Biol Chem 2004;279:40255–8.
[62] Tee MK, Rogatsky I, Tzagarakis-Foster C, Cvoro A, An J, Christy RJ, et al. Estradiol and selective estrogen receptor modulators differentially regulate target genes with estrogen receptors alpha and beta. Mol Biol Cell 2004;15:1262–72.
[63] Nakamura E, Kadomatsu K, Yuasa S, Muramatsu H, Mamiya T, Nabeshima T, et al. Disruption of the midkine gene (Mdk) resulted in altered expression of a calcium binding protein in the hippocampus of infant mice and their abnormal behaviour. Genes Cells 1998;3:811–22.
[64] Liedert A, Mattausch L, Rontgen V, Blakytny R, Vogele D, Pahl M, et al. Midkine-deficiency increases the anabolic response of cortical bone to mechanical loading. Bone 2011;48:945–51.
[65] Surjit M, Ganti KP, Mukherji A, Ye T, Hua G, Metzger D, et al. Widespread negative response elements mediate direct repression by agonist-liganded glucocorticoid receptor. Cell 2011;145:224–41.

Journal of Steroid Biochemistry & Molecular Biology 127 (2011) 301–306

Contents lists available at ScienceDirect

Journal of Steroid Biochemistry and Molecular Biology

journal homepage: www.elsevier.com/locate/jsbmb

Androgen dependent transcription of a mouse prostatic protein gene, PSP94: Involvement of estrogen receptors☆

Nariaki Fujimoto[a,*], Shigeyuki Kitamura[b], Jun Kanno[c]

[a] Department of Disease Model, Research Institute for Radiation Biology and Medicine (RIRBM), Hiroshima University, 1-2-3 Kasumi, Minami-ku, Hiroshima 734-8553, Japan
[b] Faculty of Pharmacology, Nihon Pharmaceutical University, 10281 Komuro, Inamachi, Kita-ashikaga-gun, Saitama 362-0806, Japan
[c] Division of Toxicology, Biological Safety Research Center, National Institute of Health Sciences, Kamiyoga 1-18-1, Setagaya-ku, Tokyo 158-8501, Japan

ARTICLE INFO

Article history:
Received 20 April 2011
Received in revised form 20 July 2011
Accepted 2 August 2011

Keywords:
PSP94
Androgen dependent transcription
ARE
Androgen receptor
Estrogen receptor

ABSTRACT

Prostatic secretory protein 94 (PSP94) is a prostatic protein found in both humans and rodents. As with other prostatic proteins, expression of this protein is regulated by androgens. In order to understand the androgen-responsive transcriptional regulation mechanisms involved, the present study aimed to identify and characterize the promoter activity of the gene. The 5′flanking (5′f) region of mouse PSP94 (mPSP94) gene was cloned and introduced into a vector upstream of the luciferase reporter gene. A Chinese hamster ovarian cell line, CHO, and a human prostate adenocarcinoma cell line, LNCaP, were transiently transfected with our reporter constructs along with an androgen receptor expression vector, and treated with dihydrotestosterone. Reporter gene assay revealed that the 5′f region of mPSP94 gene was indeed responsible for the androgen-dependent transcription. Subsequent deletion and mutation analysis indicated that the androgen responsive element (ARE)-like sequence at position −93 from the transcription start site was primarily responsible for androgen dependency. Interestingly, when estrogen receptor (ER) α was co-transfected, the androgen-dependent transcription was substantially increased. However, ERα-dependent enhancement of androgen responses was not observed when estrogen responsive element (ERE)-like motifs of the promoter region were deleted. Administration of estrogen did not influence the enhancement associated with ERα, although an anti-estrogen suppressed such effects. Collectively, these data suggest that the androgen-dependent transcription of the mPSP94 gene was co-regulated/modulated by the presence of ERα via ERE-like motifs.

1. Introduction

Prostatic secretory protein 94 (PSP94), or β-microseminoprotein, is one of the major proteins along with PSA (prostate specific antigen) and PAP (prostatic acid phosphatase) that are secreted by the human prostate gland [1–3]. PSP94 is also secreted in abundance by the rodent prostate although the composition of prostatic proteins differ significantly between rodents and primates [4,5]. The rodent prostate consists of anatomically separate prostatic lobes including ventral, lateral, dorsal and anterior lobes. PSP94 is known to be highly expressed in dorsal and lateral regions of the rat prostate but localized to ventral and dorso-lateral prostatic lobes in mice. PSP94 may function as an immunoglobulin binding protein and is involved in the regulation of immune response in the female reproductive tract [6]. In addition, PSP94 is known to inhibit motility of sperm and the acrosome reaction [7]. PSP94 homologues have been identified in several other mammals and non-mammalian species including ostrich and Japanese viper [8]. The PSP94 family of proteins share ten highly conserved cysteine residues.

The expression of PSP94 is regulated by androgens, in a manner similar to other prostatic proteins such as human PSA and rat probasin [9–11]. In the human PSA gene, an androgen-responsive element (ARE) motif capable of inducing transcription in response to androgens via androgen receptors (AR) was identified in the promoter region at position −156 upstream of the transcriptional starting site [12]. Another functional ARE was additionally identified at approximately −4 kbp [13]. In the rat probasin gene, two functional AREs were identified in the 5′flanking (5′f) region. Interestingly, these were androgen selective AREs rather than responsive to androgens and glucocorticoids [14,15]. In the case of PSP94, it was demonstrated that the 5′f region of the mouse PSP94 (mPSP94) gene exhibited promoter activity which conferred prostatic-specific expression in transgenic mice [16]. However, the androgen-responsive transcription mechanism responsible for such promoter activity has yet to be identified.

☆ Grant support: Grant-in-Aid (H19-kagaku-Ippan-003) from the Ministry of Health, Labor and Welfare, Japan; Grant-in-Aid (#17510046) from the Ministry of Education, Culture, Sports, Science and Technology, Japan.
* Corresponding author. Tel.: +81 82 257 5820; fax: +81 82 256 7107.
E-mail address: nfjm@hiroshima-u.ac.jp (N. Fujimoto).

0960-0760/$ – see front matter © 2011 Elsevier Ltd. All rights reserved.
doi:10.1016/j.jsbmb.2011.08.001

At position −93 from the transcription start site of mPSP94 gene, there is an ARE-like sequence, TACCTAnnnTGTTCT that contains half site of consensus ARE, TGTTCT. We demonstrated that this site is indeed a functional ARE for androgen-dependent transcription in the present study. Interestingly, the promoter region also contains sequences similar to estrogen responsive element (ERE) which enhance androgen-dependent promoter activity of the gene in the presence of the estrogen receptor (ER) α.

2. Materials and methods

2.1. Construction of reporter plasmids and transient transfection

The 5′f region of the mPSP94 gene (GenBank AF087140) was cloned by precise PCR. Specific primers at positions −1202 and +21 from the transcription start site were designed (5′-AGCAACCTCACTTGTTCCTCAGA and 5′-GGTACCTCCAGCAAAGTCCTTG). PCR was performed with PrimStar Taq (Takara Bio., Otsu, Japan) and genomic DNA of C57BL mouse liver following the manufacturer's recommended conditions. After adding an adenosine residue, the PCR fragment was cloned into the pCR2.1-TOPO TA cloning vector (Invitrogen, Carlsbad, CA, U.S.A.) and the sequence confirmed with a capillary sequencer, ABI PRISM 310 (Applied Biosystems, Foster City, CA, U.S.A.). Truncated fragments of the 5′f region were also prepared by PCR with LA-Taq (Takara Bio.) between positions −450, −358, −200, −118, −95, −76 and +21 from the cloned 5′f region −1202/+21. Each fragment was cloned into the PCR2.1-TOPO vector. Sac I/Xho I-digested fragments were then inserted into the corresponding restriction enzyme sites of the pGL3-basic luciferase reporter plasmid (Promega, Madison, WI, U.S.A.), and designated as mPSP94p-1202, -450, -358, -200, -118, -95, -76.

Mutations and deletions were introduced into pGL3 promoters using a QuickChange Site-Directed Mutagenesis Kit (Agilent Technology, Santa Clara, CA, U.S.A.). For ARE analysis, nucleotides between positions −85 and −79, and between −44 and −31 were deleted from mPSP94p-118. In addition, the TGT sequence at position −84 was changed to GAG. For ERE analysis, estrogen responsive element (ERE)-like sequences between positions −435/−421 and −216/−202 were deleted from the PSP94p-450 reporter. Construction of the hAR and hER expression plasmids, pSG5-hAR, pSG5-hERα, pSG5-hERβ were as described previously [17]. PhRL-CMV (Promega) was utilized as an internal control.

CHO cells were plated at a concentration of 2×10^4/well in 48-well plates and transiently transfected with 300 ng of a reporter, 30 ng of pSG5-hAR and 2 ng of phRL-CMV with Hilymax transfection reagent containing a synthetic cationic lipid (Dojindo Laboratories, Kumamoto, Japan), following the manufacturer's protocol. The weight ratio of the reagent to DNA was 1:1. After 24 h of incubation, cells were harvested with 25 μl of cell lysis buffer (Promega) and firefly and renilla luciferase activities determined with a Dual Luciferase Assay Kit (Promega) by measuring luminescence with a Lumino/Fluro meter. Firefly luciferase reporter activity was normalized to renilla luciferase activity from phRL-CMV. For transfection into the LNCaP cell line, a concentration of 4×10^4 cells was plated into 48-well plates; the ratio of reagent to DNA was 3:1.

DNA motif searches for ARE and ERE were performed using TRANSFAC at http://www.genome.jp/tools/motif/.

2.2. Cell culture

The CHO cell line was maintained in DME medium (Sigma Chemical Co., St. Louis, Mo., U.S.A.) containing penicillin and streptomycin with 5% FBS (Biosolutions Japan Co., Osaka, Japan). The LNCaP cell line was maintained in RPMI-1640 medium (Sigma Chemical Co.) with 10% FBS and penicillin/streptomycin. For hormone treatment experiments, cells were maintained for a week in phenol red-free medium (Sigma Chemicals) containing the same antibiotics along with dextran-charcoal treated sera. Dihydrotestosterone (DHT), hydroxy flutamide (OH-flutamide), 17β-estradil (E_2) and ICI182780 were purchased from Wakojunyaku K.K., Osaka, Japan, Toronto Research Chemicals Inc., North York, ON, Canada, Sigma Chemicals and Tocris Bioscience, Ellisville, MI, U.S.A., respectively.

3. Results

3.1. DHT-dependent promoter activity of the 5′f region of mPSP94 gene

Data concerning promoter activity of the cloned 5′f region −1202/+21 and the successive truncated regions in response to DHT are summarized in Fig. 1A. Position numbers are assigned based upon the transcription start site (+1). Significant induction of luciferase activity by DHT was noted in all constructs but mPSP94p-76, which suggested that the region between positions −95 and −76 was essential for androgen-dependent transcription. The induction appeared lower with reporter constructs containing longer distal 5′f regions of the promoter, although these remained significant in terms of induction.

Since there is a half conserved ARE sequence between positions −84 and −79, luciferase activities of the mPSP94p-118 reporter deleting this region and a reporter exhibiting mutations within this site converting TGT to GAG at position −84 were examined and are shown in Fig. 1B. Those constructs disrupting the half ARE site showed no induction of luciferase activity in response to DHT, while a reporter constructing deleting elsewhere (Δ-44/-31) exhibited DHT-dependent transcription.

Induction of mPSP94p-118 reporter activity was DHT-dependent, and significant responses were identified with 10^{-11} M of DHT with maximal response at 10^{-9} M (Fig. 1C). An anti-androgen, OH-flutamide, antagonized the DHT-induced responses (Fig. 1D).

3.2. Enhancement of DHT responsive transcription in the presence of ERα

The observed increase in mPSP94-p1202 activity treated with DHT at 10^{-9} M was about 2.5 fold of the control, which was lower than that with mPSP94p-118. When an ERα expression vector was co-transfected in CHO cells along with the AR expression vector, the mPSP94p-1202 reporter activity in response to DHT increased significantly, but did not alter PSP94-p118-luc activity. Increased levels of ERα transfection resulted in higher PSP94-1202 activity in response to androgens (Fig. 2A). Transfection of ERβ, on the other hand, did not alter response to androgens. ICI 182780 suppressed the androgen-induced promoter activity of mPSP94 while E_2 administration did not alter activity (Fig. 2B).

3.3. ERE-like motifs in the 5′f region of mPSP94 gene

The enhancing effects of ERα were examined with successive truncated luciferase reporters (Fig. 3A). Significant enhancement was observed with PSP94p-1202 and -450 but not with -200 or -118. Since there are two ERE-like motifs at positions −435 and −216 in the promoter region, it is possible that these sequences may be involved in the ER-dependent enhancement of testosterone responses. When both ERE-like motifs were deleted in the PSP94p-450 reporter, the expected enhancement with ERα was lost, while deletions of only one of the EREs did not affect the enhancing effect (Fig. 3B).

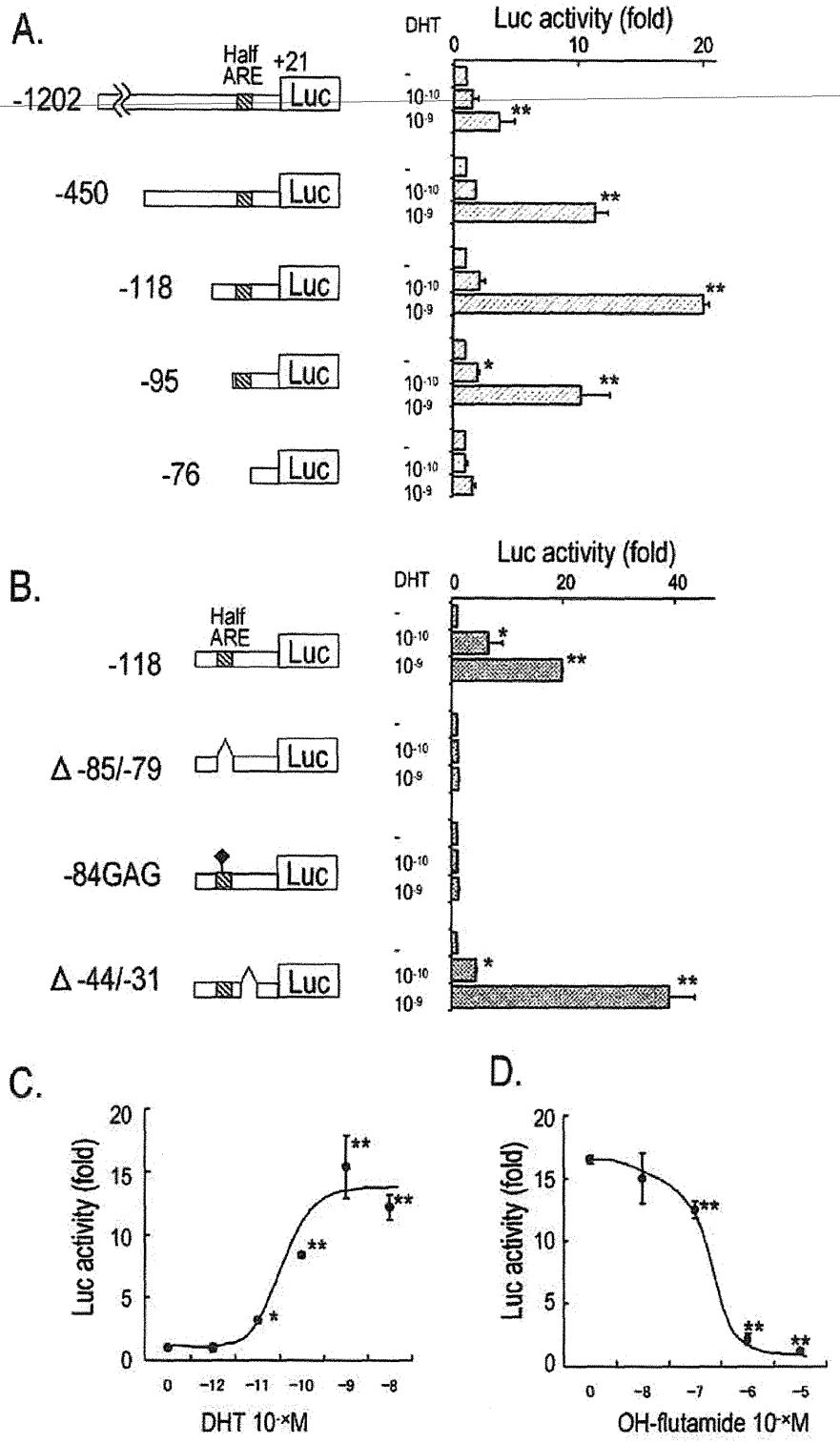

Fig. 1. DHT-dependent promoter activity of the mPSP94 gene in CHO cells. (A) Successive truncated fragments of the 5′f region from mPSP94 were inserted into a luciferase reporter. Position numbers were assigned based on the transcription start site (+1). Reporter plasmids (300 ng) and 30 ng of pSG5-hAR were transfected. DHT was administered at concentrations of 10^{-10} and 10^{-9} M. (B) DHT-induced luciferase activities of deletion and point mutants from the mPSP94p-118 reporter. (C) DHT-dose dependent induction of luciferase activity from the mPSP94p-118 reporter. (D) Dose dependent inhibition by OH-flutamide against DHT (10^{-9} M) induced activity. Bar indicates mean ± SEM, $n = 5$. $^{*}p < 0.05$ and $^{**}p < 0.01$ vs. control.

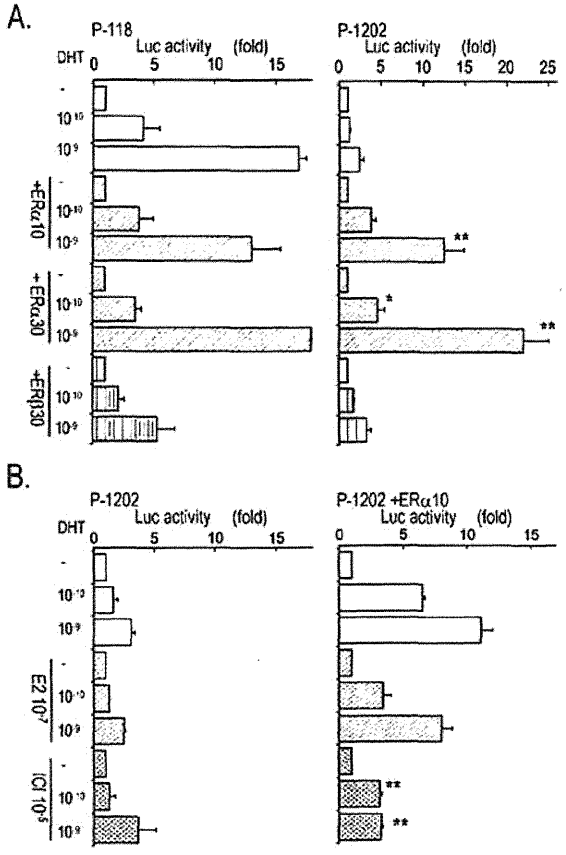

Fig. 2. Effects of ERα transfection upon DHT-dependent promoter activity of the mPSP94 gene in CHO cells. (A) Reporters containing p-118 or p-1202 were transfected along with 30 ng of pSG5-hAR and/or pSG5-hERα (10 or 30 ng) or pSG5-hERβ (30 ng). DHT was administered at concentrations of 10^{-10} or 10^{-9} M. (B) A reporter containing p-1202, pSG5-hAR and/or pSG5-hERα were transfected. DHT was administered at concentrations of 10^{-10} or 10^{-9} M with/without estradiol (E2) at 10^{-7} or ICI182178 at 10^{-5} M. Bar indicates mean ± SEM, $n=5$. *$p<0.05$ and **$p<0.01$ vs. control.

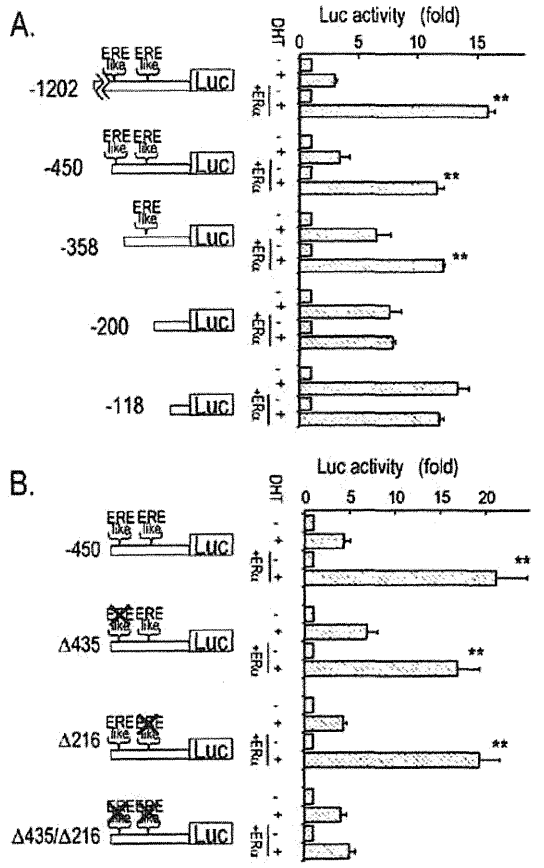

Fig. 3. Requirement of ERE-like motifs for ERα-dependent enhancing effects of androgen responses of the mPSP94 gene in CHO cells. (A) Successive truncated fragments of the mPSP94 promoter were transfected along with pSG5-hAR and pSG5-hERα. DHT was at 10^{-9} M. (B) Deletion mutants of pGL3-mPSP94p-450 were transfected with pSG5-hAR and pSG5-hERα. Bar indicates mean ± SEM, $n=5$. *$p<0.05$ and **$p<0.01$ vs. ER negative control.

3.4. Promoter activity in LNCaP cells

Responses of reporter genes to DHT with successive truncated fragments of the mPSP94 promoter in the LNCaP cell line are summarized in Fig. 4A. Significant inductions were noted in all reporter constructs except mPSP94p-76. We also examined the effect of co-transfection with an ERα expression vector (Fig. 4B). With the mPSPp-118 reporter, ERα did not alter DHT responses, while mPSP94p-450 responses were significantly increased by co-transfection with the ERα expression vector. Co-transfection with the ERα expression vector did not change the response of mPSPp-450(Δ435/Δ216).

4. Discussion

PSP94 is a non-glycosylated and cysteine-rich protein composed of 94 amino acids [3,18,19]. First isolated from human seminal plasma, PSP94 was found to be one of the major prostatic proteins in humans [1]. Although the composition of rodent prostatic proteins is very different from that of humans, PSP94 is commonly expressed in rodents [5,20]. The function of this protein has yet to be fully determined. PSP94 exhibits immunoglobulin-binding capability in order to suppress the activation of B cells [7]. PSP94 may also function as an inhibitor of sperm motility [8].

Prostatic proteins are generally regulated by androgens. When the expression of proteins secreted from the mouse prostate was examined in our previous study, we found that all proteins were indeed significantly reduced just one week following castration of the animal but increased following androgen administration [21]. Some genes may be regulated by the direct interaction of liganded AR and promoter/enhancer regions of the gene, while other changes would be secondary or tertiary events along with involution and regeneration of the prostate tissue. In the case of PSP94, testosterone administration increased mRNA levels in castrated mice by a factor of 38 in just 24 h, suggesting that gene expression was directly controlled by androgens. PSP94 mRNA is expressed in ventral prostate as well as dorso-lateral prostate in the mouse, but is localized specifically in the dorso- and lateral-prostate lobes in the rat. In humans, the expression of PSP94 was not restricted to the prostate but was additionally detected in secretions from the respiratory tract, gastric fluid and other secretory tissues [18]. Since expression was very specific to the prostate in rodents, the promoter/enhancer structure of mPSP94 gene has drawn significant interest as potential gene targeting tools. It has been demonstrated that a 3.8 kb of the 5′f region was capable of directing gene expression in a prostate tissue specific mode, that was additionally ventral- and dorso-lateral lobe specific, in a transgenic mouse model [16].

Androgens regulate their responsive genes via intracellular ARs. Upon ligand binding, ARs interact with specific DNA sequences,

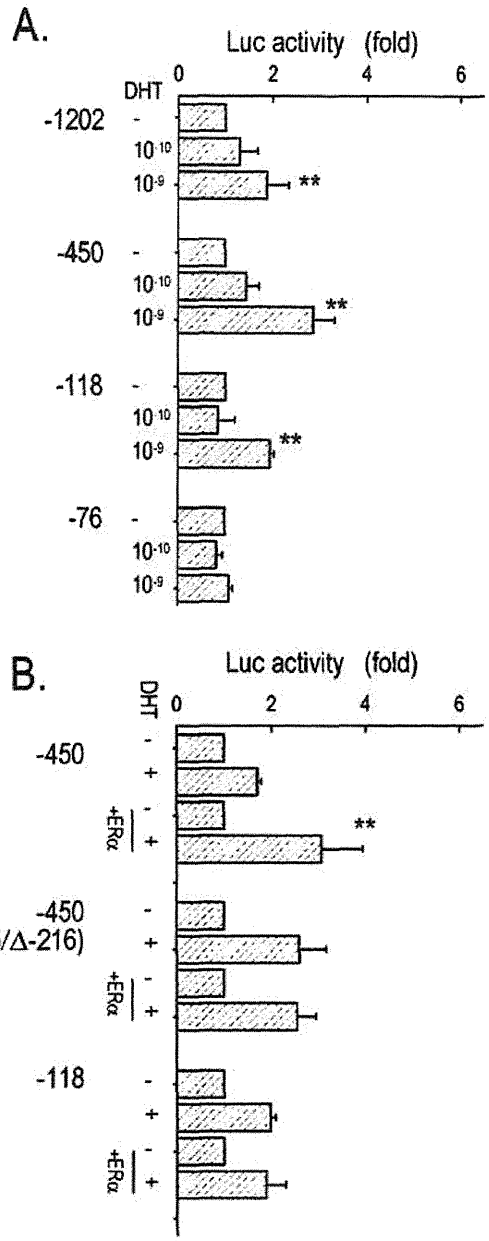

Fig. 4. DHT-dependent promoter activity of the mPSP94 gene in LNCaP cells. (A) Luciferase reporter constructs containing truncated fragments of the mPSP94 promoter were transfected and DHT was administered at concentrations of 10^{-10} and 10^{-9} M. (B) Reporter constructs containing p-450, ERE deleted p-450(Δ435/Δ 216) and p-118 were transfected with pSG5-hERα. DHT was at 10^{-9} M. Bar indicates mean ± SEM, $n = 5$. $^{**}p < 0.01$ vs. DHT negative control (A) and vs. ERα negative control (B).

known as AREs, and thus regulate the transcriptional activity of genes [22,23]. Steroid hormone receptors generally bind to DNA elements consisting of inverted repeats of six base pairs by three nucleotide spacers. The consensus hexametric sequence for AR is TGTTCT, which is identical to the glucocorticoid and progesterone responsive element. Previous investigations have revealed that AREs are divided into two categories; one interacts with glucocorticoids, mineralocorticoids and progesterone receptors, in addition to ARs, while the other is specific to ARs [24,25]. Previously described sequence data suggested that AR specific AREs tend to be organized as partial direct repeats rather than inverted repeats of the consensus hexametric repeat [22]. In mPSP94, we found an ARE candidate, TACCTAnnnTGTTCT that contains a half consensus ARE at position −93. Since androgen-dependent luciferase reporter activity was completely lost when this element was deleted or mutated, this motif between positions −93 and −79 appears to represent the functional ARE, although further studies are needed to determine if there are any direct interactions between this ARE-like sequence and AR. In the present study we primarily utilized CHO cells for the promoter assay since it is easy to perform transient transfection experiments in high efficiencies with this mammalian cell line. In addition, we used LNCaP, a human prostate adenocarcinoma cell line, to confirm the biological relevance of the promoter activity. LNCaP is an AR positive cell line that grows responding to testosterone and has been frequently used to study the androgen responsive gene regulation [26].

It has been demonstrated that combined administration of androgen and estrogen synergistically enhanced the development of prostatic hyperplasia and cancer in Noble rats as well as in chemical carcinogen-treated F344 rats [27,28]. In the previous study, we examined the expression of prostatic protein genes such as probasin and kallikrein S3 to understand the molecular mechanism underling the androgen plus estrogen effect [29]. We found that estradiol enhanced the androgen dependent expression of prostatic genes along with increase in ERα expression, which suggested that the elevated prostatic ERα may contribute to the enhancing effects. In the present study, we tested this hypothesis with PSP94 promoter and found that the androgen-dependent induction was enhanced by the presence of ERα while administration of estradiol did not change the transcription levels. In the PSP94 promoter, there are two ERE-like motifs that potentially interact with ERs at positions −435 and −216, ctannAnnnTGACCT and gGGnncnnnT-GACCa, where the consensus ERE is ARGnnAnnnTGACCY. Results arising from deletion mutants indicated that at least one ERE similar motif is enough for the enhancement of androgen responses. These enhanced responses, however, did not exceed the degree of responses with the mPSP94p-118 reporter. Since reporters containing longer 5′f region displayed lower responses, it appears that the distal region of the promoter has suppressive function on the transcription and the presence of ERα may release the suppression. In normal adult prostate tissue, ERα expression is localized to stromal cells and ERβ is in epithelia [30]. In PC, however, epithelial expression of ERα increases while ERβ expression is reduced or lost [31–33]. During the development of PC, increasing ERα expression might enhance some critical androgen responsive genes related to prostatic carcinogenesis by the similar mechanisms found in the present study.

References

[1] P.A. Abrahamsson, H. Lilja, Three predominant prostatic proteins, Andrologia 22 (Suppl. 1) (1990) 122–131.
[2] J. Tremblay, G. Frenette, R.R. Tremblay, A. Dupont, M. Thabet, J.Y. Dube, Excretion of three major prostatic secretory proteins in the urine of normal men and patients with benign prostatic hypertrophy or prostate cancer, Prostate 10 (1987) 235–243.
[3] S. Garde, J.E. Fraser, N. Nematpoor, R. Pollex, C. Morin, A. Forte, S. Rabbani, C. Panchal, M.B. Gupta, Cloning expression, purification and functional characterization of recombinant human PSP94, Protein Expr. Purif. 54 (2007) 193–203.
[4] Y. Imasato, T. Onita, M. Moussa, H. Sakai, F.L. Chan, J. Koropatnick, J.L. Chin, J.W. Xuan, Rodent PSP94 gene expression is more specific to the dorsolateral prostate and less sensitive to androgen ablation than probasin, Endocrinology 142 (2001) 2138–2146.
[5] A. Thota, M. Karajgikar, W. Duan, M.Y. Gabril, F.L. Chan, Y.C. Wong, H. Sakai, J.L. Chin, M. Moussa, J.W. Xuan, Mouse PSP94 expression is prostate tissue-specific as demonstrated by a comparison of multiple antibodies against recombinant proteins, J. Cell Biochem. 88 (2003) 999–1011.
[6] M. Kamada, H. Mori, N. Maeda, S. Yamamoto, K. Kunimi, M. Takikawa, M. Maegawa, T. Aono, S. Futaki, S.S. Koide, beta-Microseminoprotein/prostatic secretory protein is a member of immunoglobulin binding factor family, Biochim. Biophys. Acta 1388 (1998) 101–110.

[7] A. Kumar, D.D. Jagtap, S.D. Mahale, M. Kumar, Crystal structure of prostate secretory protein PSP94 shows an edge-to-edge association of two monomers to form a homodimer, J. Mol. Biol. 397 (2010) 947–956.
[8] N. Aoki, A. Sakiyama, M. Deshimaru, S. Terada, Identification of novel serum proteins in a Japanese viper: homologs of mammalian PSP94, Biochem. Biophys. Res. Commun. 359 (2007) 330–334.
[9] R.J. Matusik, C. Kreis, P. McNicol, R. Sweetland, C. Mullin, W.H. Fleming, J.G. Dodd, Regulation of prostatic genes: role of androgens and zinc in gene expression, Biochem. Cell Biol. 64 (1986) 601–607.
[10] K.B. Cleutjens, C.C. van Eekelen, H.A. van der Korput, A.O. Brinkmann, J. Trapman, Two androgen response regions cooperate in steroid hormone regulated activity of the prostate-specific antigen promoter, J. Biol. Chem. 271 (1996) 6379–6388.
[11] Z. Wang, R. Tufts, R. Haleem, X. Cai, Genes regulated by androgen in the rat ventral prostate, Proc. Natl. Acad. Sci. U.S.A. 94 (1997) 12999–13004.
[12] P.H. Riegman, R.J. Vlietstra, J.A. van der Korput, A.O. Brinkmann, J. Trapman, The promoter of the prostate-specific antigen gene contains a functional androgen responsive element, Mol. Endocrinol. 5 (1991) 1921–1930.
[13] S. Zhang, P.E. Murtha, C.Y. Young, Defining a functional androgen responsive element in the 5′ far upstream flanking region of the prostate-specific antigen gene, Biochem. Biophys. Res. Commun. 231 (1997) 784–788.
[14] S. Kasper, P.S. Rennie, N. Bruchovsky, L. Lin, H. Cheng, R. Snoek, K. Dahlman-Wright, J.A. Gustafsson, R.P. Shiu, P.C. Sheppard, R.J. Matusik, Selective activation of the probasin androgen-responsive region by steroid hormones, J. Mol. Endocrinol. 22 (1999) 313–325.
[15] P.S. Rennie, N. Bruchovsky, K.J. Leco, P.C. Sheppard, S.A. McQueen, H. Cheng, R. Snoek, A. Hamel, M.E. Bock, B.S. MacDonald, Characterization of two cis-acting DNA elements involved in the androgen regulation of the probasin gene, Mol. Endocrinol. 7 (1993) 23–36.
[16] M.Y. Gabril, T. Onita, P.G. Ji, H. Sakai, F.L. Chan, J. Koropatnick, J.L. Chin, M. Moussa, J.W. Xuan, Prostate targeting: PSP94 gene promoter/enhancer region directed prostate tissue-specific expression in a transgenic mouse prostate cancer model, Gene Ther. 9 (2002) 1589–1599.
[17] S. Kitamura, T. Suzuki, S. Ohta, N. Fujimoto, Antiandrogenic activity and metabolism of the organophosphorus pesticide fenthion and related compounds, Environ. Health Perspect. 111 (2003) 503–508.
[18] J.W. Xuan, D. Wu, Y. Guo, S. Garde, D.T. Shum, M. Mbikay, R. Zhong, J.L. Chin, Molecular cloning and gene expression analysis of PSP94 (prostate secretory protein of 94 amino acids) in primates, DNA Cell Biol. 16 (1997) 627–638.
[19] J.W. Xuan, J. Kwong, F.L. Chan, M. Ricci, Y. Imasato, H. Sakai, G.H. Fong, C. Panchal, J.L Chin, cDNA, genomic cloning, and gene expression analysis of mouse PSP94 (prostate secretory protein of 94 amino acids), DNA Cell Biol. 18 (1999) 11–26.
[20] J. Kwong, J.W. Xuan, H.L. Choi, P.S. Chan, F.L. Chan, PSP94 (or beta-microseminoprotein) is a secretory protein specifically expressed and synthesized in the lateral lobe of the rat prostate, Prostate 42 (2000) 219–229.
[21] N. Fujimoto, Y. Akimoto, T. Suzuki, S. Kitamura, S. Ohta, Identification of prostatic-secreted proteins in mice by mass spectrometric analysis and evaluation of lobe-specific and androgen-dependent mRNA expression, J. Endocrinol. 190 (2006) 793–803.
[22] F. Claessens, S. Denayer, N. Van Tilborgh, S. Kerkhofs, C. Helsen, A. Haelens, Diverse roles of androgen receptor (AR) domains in AR-mediated signaling, Nucl. Recept. Signal. 6 (2008) e008.
[23] E.C. Bolton, A.Y. So, C. Chaivorapol, C.M. Haqq, H. Li, K.R. Yamamoto, Cell- and gene-specific regulation of primary target genes by the androgen receptor, Genes Dev. 21 (2007) 2005–2017.
[24] P.S. Nelson, N. Clegg, H. Arnold, C. Ferguson, M. Bonham, J. White, L. Hood, B. Lin, The program of androgen-responsive genes in neoplastic prostate epithelium, Proc. Natl. Acad. Sci. U.S.A. 99 (2002) 11890–11895.
[25] F. Claessens, G. Verrijdt, E. Schoenmakers, A. Haelens, B. Peeters, G. Verhoeven, W. Rombauts, Selective DNA binding by the androgen receptor as a mechanism for hormone-specific gene regulation, J. Steroid Biochem. Mol. Biol. 76 (2001) 23–30.
[26] J. Veldscholte, C.A. Berrevoets, E. Mulder, Studies on the human prostatic cancer cell line LNCaP, J. Steroid Biochem. Mol. Biol. 49 (1994) 341–346.
[27] R.L. Noble, The development of prostatic adenocarcinoma in Nb rats following prolonged sex hormone administration, Cancer Res. 37 (1977) 1929–1933.
[28] K. Suzuki, Y. Takezawa, T. Suzuki, S. Honma, H. Yamanaka, Synergistic effects of estrogen with androgen on the prostate—effects of estrogen on the prostate of androgen-administered rats and 5-alpha-reductase activity, Prostate 25 (1994) 169–176.
[29] N. Fujimoto, H. Honda, T. Suzuki, S. Kitamura, Estrogen enhancement of androgen-responsive gene expression in hormone-induced hyperplasia in the ventral prostate of F344 rats, Cancer Sci. 95 (2004) 711–715.
[30] T. Tsurusaki, D. Aoki, H. Kanetake, S. Inoue, M. Muramatsu, Y. Hishikawa, T. Koji, Zone-dependent expression of estrogen receptors alpha and beta in human benign prostatic hyperplasia, J. Clin. Endocrinol. Metab. 88 (2003) 1333–1340.
[31] G.S. Yang, Y. Wang, P. Wang, Z.D. Chen, Expression of oestrogen receptor-alpha and oestrogen receptor-beta in prostate cancer, Chin. Med. J. (Engl.) 120 (2007) 1611–1615.
[32] M. Royuela, M.P. de Miguel, F.R. Bethencourt, M. Sanchez-Chapado, B. Fraile, M.I. Arenas, R. Paniagua, Estrogen receptors alpha and beta in the normal, hyperplastic and carcinomatous human prostate, J. Endocrinol. 168 (2001) 447–454.
[33] L.G. Horvath, S.M. Henshall, C.S. Lee, D.R. Head, D.I. Quinn, S. Makela, W. Delprado, D. Golovsky, P.C. Brenner, G. O'Neill, R. Kooner, P.D. Stricker, J.J. Grygiel, J.A. Gustafsson, R.L. Sutherland, Frequent loss of estrogen receptor-beta expression in prostate cancer, Cancer Res. 61 (2001) 5331–5335.

Biochemical and Biophysical Research Communications 412 (2011) 366–372

Contents lists available at ScienceDirect

Biochemical and Biophysical Research Communications

journal homepage: www.elsevier.com/locate/ybbrc

Genistein promotes DNA demethylation of the steroidogenic factor 1 (SF-1) promoter in endometrial stromal cells

Hiroshi Matsukura [a], Ken-ichi Aisaki [b], Katsuhide Igarashi [b], Yuko Matsushima [b], Jun Kanno [b], Masaaki Muramatsu [a], Katsuko Sudo [a,c], Noriko Sato [a,*]

[a] Department of Molecular Epidemiology, Medical Research Institute, Tokyo Medical and Dental University, 2-3-10 Kanda-surugadai, Chiyoda-ku, Tokyo 101-0062, Japan
[b] Division of Cellular and Molecular Toxicology, National Institute of Health Sciences, 1-18-1 Kamiyoga, Setagaya-ku, Tokyo 158-8501, Japan
[c] Animal Research Center, Tokyo Medical University, 6-1-1 Shinjuku, Shinjuku-ku, Tokyo 160-8402, Japan

ARTICLE INFO

Article history:
Received 21 July 2011
Available online 29 July 2011

Keywords:
Genistein
DNA methylation
Ovariectomized mice
Primary culture
Steroidogenic factor 1
High-resolution melting analysis

ABSTRACT

It has recently been demonstrated that genistein (GEN), a phytoestrogen in soy products, is an epigenetic modulator in various types of cells; but its effect on endometrium has not yet been determined. We investigated the effects of GEN on mouse uterine cells, *in vivo* and *in vitro*. Oral administration of GEN for 1 week induced mild proliferation of the endometrium in ovariectomized (OVX) mice, which was accompanied by the induction of steroidogenic factor 1 (SF-1) gene expression. GEN administration induced demethylation of multiple CpG sites in the SF-1 promoter; these sites are extensively methylated and thus silenced in normal endometrium. The GEN-mediated promoter demethylation occurred predominantly on the luminal side, as opposed to myometrium side, indicating that the epigenetic change was mainly shown in regenerated cells. Primary cultures of endometrial stromal cell colonies were screened for GEN-mediated alterations of DNA methylation by a high-resolution melting (HRM) method. One out of 20 colony-forming cell clones showed GEN-induced demethylation of SF-1. This clone exhibited a high proliferation capacity with continuous colony formation activity through multiple serial clonings. We propose that only a portion of endometrial cells are capable of receiving epigenetic modulation by GEN.

1. Introduction

Genistein (GEN), a major phytoestrogen in dietary soy, is a substantial component of the typical Asian and Western vegetarian diets, as well as recently developed infant soy milk formulas. There are several well known potential health benefits of GEN intake [1,2], one of which is an apparent decreased risk of breast and prostate cancers, based on human observational studies [1,3]. But GEN also paradoxically stimulates growth of breast cancer cells in culture [2] and uterine enlargement in rodents [4]. These effects may be mediated through estrogen receptor interactions and/or modulation of endogenous estrogen metabolism [5,6]. Since GEN can bind to estrogen receptors (ERs) α and β, with a stronger affinity to ERβ [5], it is categorized as a phyto-selective estrogen receptor modulator (SERM) [6,7]. The variations in GEN's agonistic or antagonistic effects may be affected by variations in endogenous estrogen levels. Previous studies have not determined whether the pleiotropic effects of GEN involve distinct epigenetic alteration. Recently, GEN was shown to alter DNA methylation in various types of cells, including ES cells [8], but most studies have been performed using cancer cell lines [9–11]. There have been few reports of the effects of GEN on DNA methylation in intact cells or *in vivo* [12]. In the present study, we utilized a uterotropic assay in ovariectomized (OVX) mice, as a model system to analyze epigenetic regulation by GEN.

In a previous study, high-dose GEN administration to OVX rats resulted in increased uterine weight and changed endometrial cell gene expression [6]. However, no epigenetic alterations were demonstrated under this condition. We selected the steroidogenic factor 1 (SF-1; official symbol: Nr5a1) gene as a target for the methylation analysis. SF-1 is an orphan nuclear receptor and transcription factor for key enzymes involved in steroidogenesis, such as StAR, Cyp11a1 (p450scc), Cyp17a1 (p450c17), and Cyp19a1 (aromatase) [13]. The SF-1 gene is not expressed in normal endometrium; however, SF-1 expression is reactivated in the disease state of human ectopic endometriosis, in which the SF-1 promoter is abnormally demethylated by an unknown mechanism [14]. The subsequent enhancement of steroidogenic genes and resultant local steroidogenesis are proposed to be important etiologies [15]. Therefore, we hypothesized that in mouse endometrial cells,

* Corresponding author. Fax: +81 3 5280 8058.
E-mail addresses: hmatsukura.epi@mri.tmd.ac.jp (Hiroshi Matsukura), nsato.epi@tmd.ac.jp (N. Sato).

0006-291X/$ - see front matter © 2011 Elsevier Inc. All rights reserved.
doi:10.1016/j.bbrc.2011.07.104

SF-1 might be subjected to epigenetic modulation by some external stimuli. Here we show that the SF-1 promoter was demethylated *in vivo* and *in vitro* by GEN treatment. This is the first demonstration of a phytoestrogen altering the epigenetic state of adult endometrium.

2. Materials and methods

2.1. Ethics statement

All procedures described here were performed according to protocols approved by the Animal Care Committee of the National Institute of Health Sciences, and Tokyo Medical and Dental University (No. 0110306A).

2.2. Oral administration of genistein to ovariectomized mice

C57BL/6JJmsSlc female mice (SLC) were used in this study. All mice were fed a phytoestrogen-free diet (Oriental Yeast) and were ovariectomized (OVX) 2 weeks prior to the genistein (GEN) treatment. OVX mice were divided into three different treatment groups, each consisting of 3–5 independent replicates, which orally received low-dose GEN (60 mg/kg/day), high-dose GEN (200 mg/kg/day), or vehicle (0.5% CMC-Na (Maruishi Pharmaceutical); 5 ml/kg/day) for 1 week. At the end of treatment (9 weeks of age), all mice were euthanized by exsanguination under ether anesthesia.

2.3. Uterotrophic assay and gene expression study after oral administration of genistein

Whole uteri were harvested, blotted, and weighted. Each uterus was divided into two horns, immediately placed into 2 ml plastic tubes of RNAlater solution (Ambion), and stored at 4 °C. From each sample, one horn was processed for mRNA expression analyses; RNAlater was replaced with 1.0 ml of RLT buffer (Qiagen), and the horn was homogenized by addition of a 5 mm diameter Zirconium bead (Funakoshi) and shaking with a MixerMill 300 (Qiagen) at 20 Hz for 5 min (only the outermost row of the shaker box was used). Further sample preparation and analysis were performed as previously described [16]. mRNA expressions were analyzed using Affymetrix Murine Genome 430 2.0 GeneChips, and calculated as copy number per cell by the Percellome method [16]. The second uterine horn of each sample was subjected to genomic DNA isolation.

2.4. Isolation of colony-forming cells derived from intact uteri

Five 8- to 9-week-old C57BL/6JJmsSlc female mice (SLC) were euthanized by cervical dislocation and whole uteri were harvested. Uterine horns were collected in Dulbecco's modified Eagle's medium/Hams F-12 (DMEM/F-12; Nacalai Tesque) containing 0.05 mg/ml gentamicin (Sigma–Aldrich). Each horn was dissected longitudinally and the endometrial tissue was divided into two portions: the luminal side and the myometrium side. A single cell suspension of endometrial cells was obtained using enzymatic digestion and mechanical means adapted from Chan et al. [17]. The tissue samples were minced and dissociated in 500 µl DMEM/F-12 containing 0.12 mg/ml (0.56 Wünsch U/ml) Blendzyme 2 and 40 µg/ml deoxyribonuclease type I (both from Roche Applied Science) in a shaking incubator (~90 rpm) at 37 °C. At 15 min intervals, the digests were pipetted to promote separation and cell dissociation was monitored microscopically. After 45 min, debris was filtered out using a 40-µm sieve (BD Biosciences). The single-cell suspensions were collected in DMEM/F-12 containing 10% FBS, 0.05 mg/ml gentamicin and stored on ice. Then the sieves were backwashed, and myometrial and glandular debris were further digested to single cells for 45 min as described above. All cell suspensions were filtered as described above, and combined. To remove erythrocytes, the cells were resuspended in 500 µl of HLB solution (Immuno Biological Laboratories) and incubated for 3 min. After washing twice with PBS, viable cell numbers were counted with trypan blue (Sigma–Aldrich). Cells were seeded on gelatin (0.1%, Sigma–Aldrich)-coated dishes at various densities of 0.1–3 × 10^5 cell/60-mm dish. After 14 days, non-overlapping clones were distinguished. Primary cell clones were expanded in DMEM/F-12 containing 5% FBS (SAFC Biosciences) and 0.05–0.1 mg/ml gentamicin, on gelatin-coated dishes.

2.5. Serial cloning of colony-forming cell clones

Self renewal was assessed by serial cloning of individual clones as described by Gargett et al. [18]. Cells were seeded on gelatin-coated 100-mm dishes at 10 cells/cm^2 (600 cells/100-mm dish). Culture medium was changed every 4 days and secondary clones formed distinct colonies by 14 days after plating. Secondary clones were similarly recloned to generate tertiary clones, and were also expanded in the same manner as the primary culture.

2.6. In vitro genistein exposure to colony-forming cells

From 70 isolated cell clones, we selected 20 clones from colonies that were composed of fibroblastic-shaped, homogenous cells with an average doubling time of less than 100 h. The selected clonal cells, whose passage number was less than 10, were subjected to *in vitro* GEN exposure. Cells were seeded on gelatin-coated 60-mm dishes, treated with or without 10 µM of GEN (dissolved in dimethylsulfoxide (DMSO)) in DMEM/F-12 containing 5% FBS and 0.05 mg/ml gentamicin for 7 days. The final DMSO concentration was 0.02%. The culture medium was changed every 2 days.

2.7. Genomic DNA preparation and bisulfite sequencing

Genomic DNA was isolated using a QIAamp DNA Mini Kit (QIAGEN) and 180 ng–1 µg was subjected to sodium bisulfite modification with a EpiTect Bisulfite Kit (QIAGEN) according to manufacturer's protocols. Bisulfite sequencing primers are shown in Supplementary Table 1. PCR products were cloned into the pT7 blue T vector (Novagen) and transformed into *Escherichia coli*. Plasmid DNA from positive colonies was purified and sequenced at the Tokyo Medical and Dental University Genome Laboratory (Tokyo, Japan). Sequence and statistical analyses were performed with the QUantification tool for Methylation Analysis; http://quma.cdb.riken.jp/top/quma_main_j.html [19]. The statistical significance of the difference between two bisulfite sequence groups at each CpG site was evaluated with Fisher's exact test.

2.8. Screening of DNA methylation status by high-resolution melting assay

All assays were performed on the LightCycler 480 using the LightCycler 480 High Resolution Melting Master kit, according to the manufacturer's instructions. Primers, designed using LightCycler Probe Design Software 2.0 (All, Roche Applied Science) are shown in Supplementary Table 1. All data were analyzed using LightCycler Gene Scanning Software.

2.9. Statistical analysis

Data are shown as means ± SD. Unpaired *t*-tests were used to compare the significance between two groups. Statistical analysis

was performed using Dr. SPSS 2 for Windows. Results were considered statistically significant at a P value of <0.05.

3. Results

3.1. Effects of genistein in uteri of ovariectomized (OVX) mice

OVX mice were fed with either vehicle (control) or low (60 mg/kg) or high (200 mg/kg) doses of GEN for 7 days and blotted uterus weights were determined (Fig. 1A). Compared to the control, low-dose GEN treatment did not significantly increase the uterus weight; high-dose treatment induced a slight but significant uterus enlargement (1.4-fold of control; $P < 0.005$). We then determined the mRNA expression levels of SF-1 (Fig. 1B) and steroidogenic genes (Fig. 1C–F) by the Percellome method. The mRNA levels of these genes were very low in the endometria from control and low-dose GEN-treatment groups, but were significantly increased (still less than one copy per cell on average) in the high-dose treatment group ($P < 0.05$), indicating that high-doses of GEN induced expression of these genes. Next, we determined the methylation status of SF-1 in

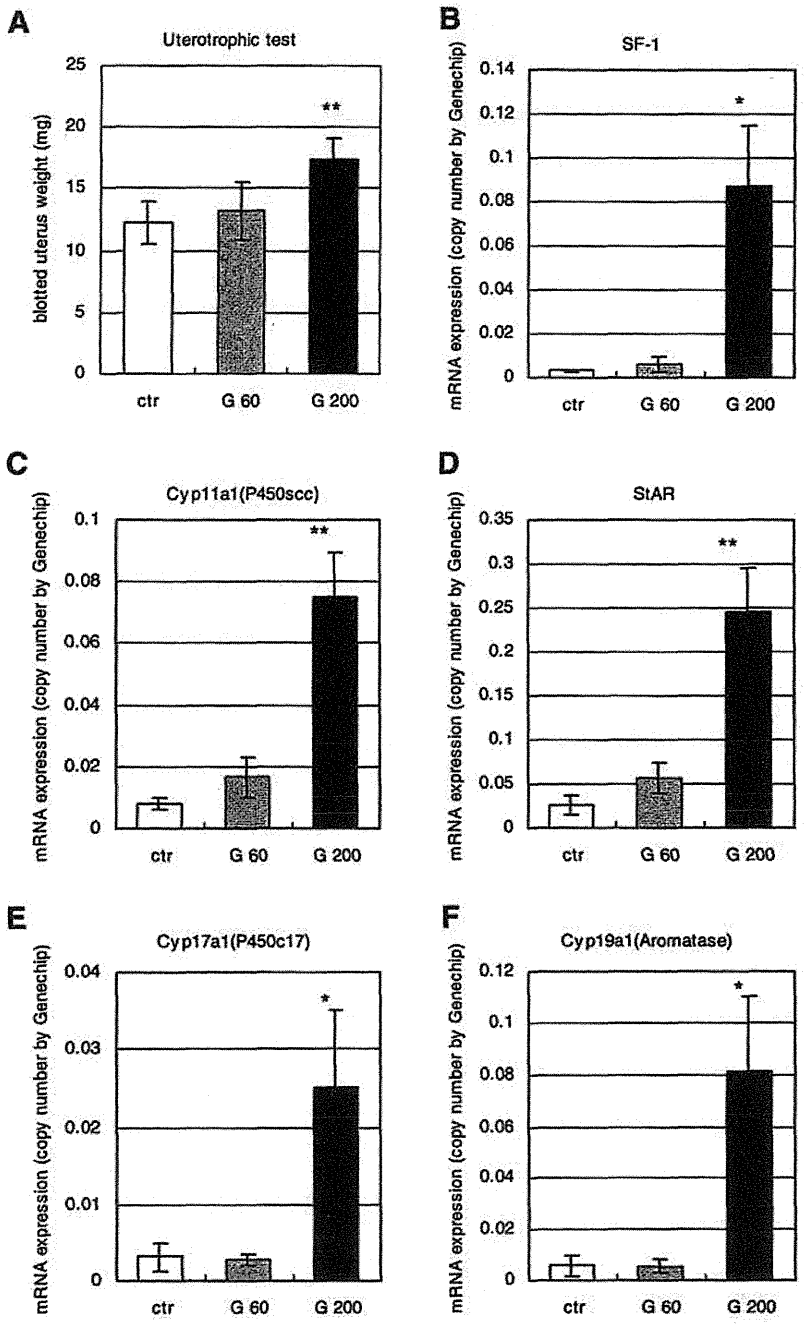

Fig. 1. Genistein induced endometrial regeneration and SF-1 mRNA expression in uterine tissue of OVX mice. (A) Blotted uterine weights were recorded. Control and GEN-treated groups comprised five and four mice, respectively. ctr; control, G 60; GEN 60 mg/kg/d, G200; GEN 200 mg/kg/d. (B–F) mRNA expressions of steroidogenic genes were determined using GeneChip analysis and were calculated by the Percellome method. *Y* axis indicates mRNA expression as copy number per cell. (B) SF-1 was determined by 1418315_at, (C) Cyp11a1 by 1439947_at, (D) StAR by 1418729_at, (E) Cyp17a1 by 1417017_at, and (F) Cyp19a1 by 1449920_at. *Statistically significant at $P < 0.05$. **Statistically significant at $P < 0.005$.